Chapter 13
Multidimensional and Comprehensive Two-Dimensional Gas Chromatography

Mohamed Adahchour and Udo A. Th. Brinkman

Contents

Abstract The analysis of many complex samples requires a performance which conventional one-dimensional (1D) GC cannot provide. In multidimensional GC (MDGC) selected fractions of the GC eluate are online subjected to a second GC separation. This is a useful technique when only one, or a few, target analyte has to be determined. When, however, wide ranging screening has to be performed or the detection/identification of unknowns is of particular interest, MDGC becomes extremely time-consuming and cannot really solve the analytical problems.

M. Adahchour (✉)
Free University, Department of Analytical Chemistry and Applied Spectroscopy, de Boelelaan 1083, NL-1081 HV Amsterdam, The Netherlands

Omegam Laboratoria B.V., H.J.E. Wenckebachweg 120, NL-1114 AD Amsterdam-Duivendrecht, The Netherlands
e-mail: m.adahchour@omegam.nl

U.A. Th. Brinkman
Free University, Department of Analytical Chemistry and Applied Spectroscopy, de Boelelaan 1083, NL-1081 HV Amsterdam, The Netherlands
e-mail: ubrinkman@hetnet.nl

K. Dettmer-Wilde and W. Engewald (eds.), *Practical Gas Chromatography*,
DOI 10.1007/978-3-642-54640-2_13,

Comprehensive two-dimensional GC (GC×GC) should now be used. Here the entire sample is subjected to two (independent) separations, using a very rapid (2–8 s) second-dimension separation in order not to lose the resolution achieved on the first column. The total run time is therefore essentially the same as with a conventional 1D separation! The set-up of a GC×GC system is discussed and attention is given to (1) the interface between the two GC columns, the (cryogenic-type) modulator, which effects the trapping of each subsequent first-column eluate fraction and its rapid relaunching onto the second column, and (2) detection, usually with a ToF MS, micro-ECD or FID detector which provide the high data acquisition rate necessary because of the fast second separation. Applications deal with the analysis of food, fragrances, biological, environmental and air/aerosol samples, and petrochemical products, and with the trace analysis of many classes of organohalogens. The much improved analyte-from-analyte as well as analytes-from-interfering background separations, the creation of 'ordered structures' which facilitate analyte classification, improved detectability, and reliable (ToF MS-based) identification are highlighted.

13.1 Multidimensional Gas Chromatography

Already in the early years of GC, it became clear that single-packed-column analyses could not provide enough efficiency to separate all analytes in a complex sample. With the advent of fused-silica capillary columns, separation power showed a dramatic increase. However, for a very large number of applications, the improved resolution merely helped to demonstrate that the actual sample complexity still could not be charted: examples include natural flavour extracts, gasoline streams, and most environmental samples. The problems are exacerbated because compounds present in (ultra-)trace amounts frequently are the species contributing most to the aroma, taste, or toxicity. Their co-elution with much larger amounts of matrix constituents poses real problems for detection, identification, and quantification. Complex samples are often loosely defined as all samples containing over about 100 compounds of interest; i.e. most real-world samples are in that category. A modern capillary column contains in excess of 100,000 plates, but already in 1990 Giddings calculated that 500 million theoretical plates would be required for a 0.99 separation probability of such a 100-component mixture [1]! Use of selective detectors will help, but the problem of obtaining clean mass spectra, the ultimate goal in many analyses, remains.

Using the consecutive separation power of two different chromatographic phases/columns has always been an attractive proposition to solve problems such as those mentioned above and, in the second half of the twentieth century, two-dimensional GC has repeatedly been shown to be an interesting technique to deal with complex samples, especially those comprising substances having a wide range of polarities. The coupled-column arrangement was the genesis of what is, today, usually called multidimensional or heart-cutting GC, the acronyms used being MDGC and GC–GC. Most developments in MDGC date back to the first decades of GC practice (with Simmons and Snyder [2] credited with the first use of

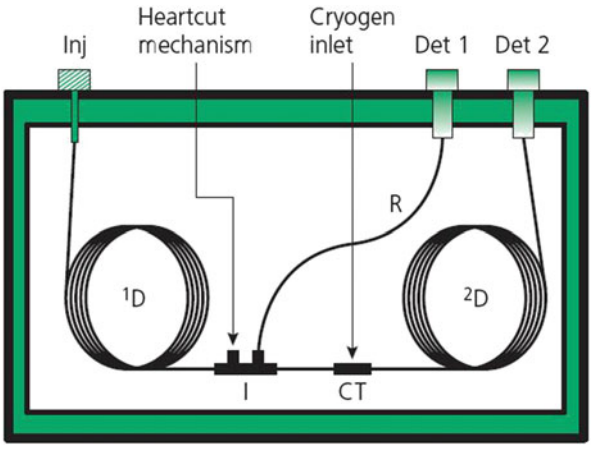

Fig. 13.1 Typical set-up of MDGC system. The basic system features an injector, two columns and two detectors housed in a single oven, a mid-point restrictor plus valve (for flow direction to waste or second column), and a cryogenic trap (for focusing of heart cuts); also see text [138]

the technique in general analysis). Review papers such as [3], [4] and [5] are relatively brief, but most useful, introductions to the technique.

Figure 13.1 presents a schematic of a typical MDGC system, comprising one oven, two columns, two detectors, and a mid-point restrictor, *I*, at which point the diversion of column flow to either the first detector, via capillary *R*, or the second column, via the cryogen inlet *CT*, occurs. A cryogenic trap focuses heart-cut fractions, and a solenoid-controlled shut-off valve closes the flow through to the monitor detector and affects the transfer of the flow of the first to the second column. Effluent-switching technologies employ either switching valves or pneumatic switching (Deans' switches). An intermediate cryogenic trap is essential whenever a band-focusing mechanism is required as part of the transfer process.

Compared to other developments in GC, over the last 20 years rather little progress has been made in the advancement of MDGC: in 1986–1998 less than 2 % of the publications in the *Chemical Abstract* database on GC was devoted to MDGC [5]. The main cause of this probably is that instrumentation for MDGC is somewhat (too) complex for acceptance in routine laboratories. The emergence of relatively low-cost and user-friendly GC–MS (using quadrupole MS, qMS, instruments) is frequently mentioned as an additional cause why MDGC has not flourished. Nevertheless, there are three areas where MDGC has made an impact, viz. (1) for the class separation, and detailed fingerprinting, of petroleum products, (2) for the separation of (poly)chlorinated biphenyls ((P)CBs) and other organochlorine compounds in environmental chemistry, and (3) in the food and fragrance industries.

In petrochemical analysis, a convincing demonstration of the separation power of MDGC was the introduction of the PIONA (paraffins/*iso*-paraffins/olefins/naphthenes/aromatics) analyser in 1971 [6]. The system comprises up to five (packed and capillary) columns—each optimized to deal with a particular range of compounds, three traps and a reactor in a set-up with six switching valves. Newer versions can handle samples having boiling points up to 270 °C [7] and can also deal with the additional separation problems caused by the introduction of oxygenates in gasoline.

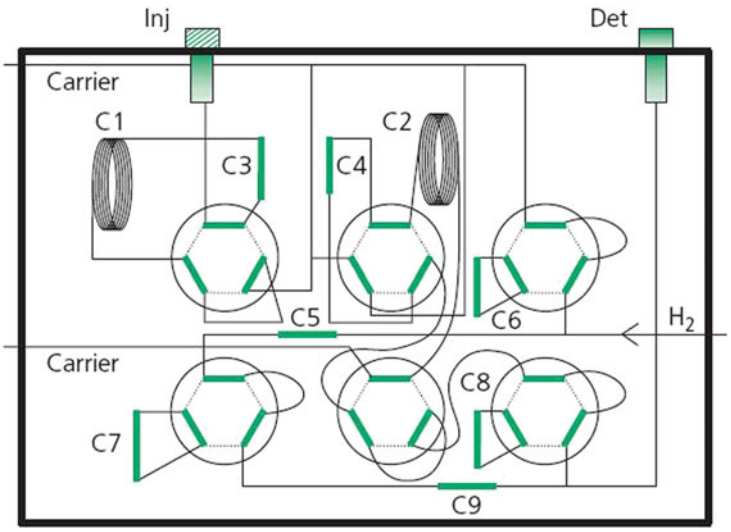

Fig. 13.2 Schematic of a PIONA system with two capillary (polar C1 and non-polar C2) and three packed (C3: alcohol retention; C8: oxygenate separation; C9: 13X mol sieve) columns, three traps to retain aromatics (C4), olefins (C6), and *n*-alkanes (C7), and an olefin hydrogenator (C5) [138]

Figure 13.2 serves to illustrate the complexity of the set-up (without providing a detailed explanation). Such an analysis, moreover, takes some 7 h.

In the mid-1990s, MDGC was called an effective technique to separate CBs and avoid interferences from other compounds [8]. However, the frequent need to take multiple heart cuts during one run was increasingly found to be a distinct disadvantage. In the analysis of food and fragrances the determination of enantiomeric ratios, i.e. the use of enantioselective MDGC in order to detect adulteration in food, was a relevant area of application. Here, the possibility to select another second GC column for each next (enantiomeric) separation problem is a major advantage of the technique.

Another topic often discussed in reviews on the applicability of MDGC is that of the complete characterization of a complex sample, with the total analysis of tobacco smoke often cited as an example. However, the reviewers invariably comment that this type of analysis cannot be addressed with any real efficiency by means of MDGC. Full characterization now requires the transfer of a very large number of individual heart cuts—a most laborious process (precise timing of the cutting events plays a crucial role) that is, moreover, extremely time-consuming because of the need to reanalyse all heart cuts individually on a second column. To give an example: taking 30-s cuts from a 45-min first-column separation will require 90 reruns of, typically, some 30 min each—which adds up to a total analysis time of 45 h! If one tries to alleviate the problem by making the individual transfers wider (e.g. 60 instead of 30 s), an essential part of the resolution achieved on the first column will be lost and the second separation will, consequently, be much less satisfactory and, still, very time-consuming.

In summary, MDGC is a technique that is well suited to separate and detect one or a few target compounds present in one or two narrow windows of a complex

chromatogram, and the technique is indeed used to this end also today. Relevant examples include [9], [10], and [11]. However, other such studies discuss rather too complex problems and would most probably profit from using the comprehensive approach.

Since MDGC cannot be used to efficiently solve problems in which total profiling of a complex sample (extract) is required, we have to return to our initial discussion and design, as an alternative to conventional GC–GC with its heart-cutting approach, a comprehensive multidimensional, or GC×GC, system, in which the entire effluent from the first (or 'first-dimension', to use the comprehensive nomenclature) column is examined by a second (second-dimension) column. This will have to be done in a continuous, real-time mode whilst maintaining essentially all of the first-dimension resolution. To put it differently, it will have to be done by taking some three or four heart cuts across each individual first-dimension peak and analyse each of these before the next heart cut arrives at the top of the second-dimension column. Here, we have defined the challenging problem that was solved, in 1991, by professor John Phillips and his group [12] and that will be the subject of the rest of this chapter.

13.2 Comprehensive Two-Dimensional Gas Chromatography

The powerful alternative to the problem sketched above is to subject a sample to a comprehensive two-dimensional (2D), or GC×GC, separation. Rather than a few selected fractions, the entire sample is now subjected to a separation on two different GC columns, the fractions are kept sufficiently narrow to ensure that no information gained during the first separation is lost, and the instrumental set-up is constructed so as to ensure that the total 2D separation is completed within the run time of the first-dimension analysis. In other words, GC×GC aims at yielding improved resolution for *all* instead of *a few selected* sample constituents, and this should be effected without any real loss of time compared with a conventional 1D-GC analysis. In the present chapter, attention will be devoted to (1) the general set-up of GC×GC systems and (2) the coupling of GC×GC systems with a variety of GC detectors.

13.2.1 Instrumental Set-Up

The GC×GC system From a practical point of view, it suffices to repeat that in GC×GC an entire sample is subjected to two GC separations which are based on different separation mechanisms. A schematic of such a system is shown in Fig. 13.3; next to an injection and a detection system, and the two GC columns, it

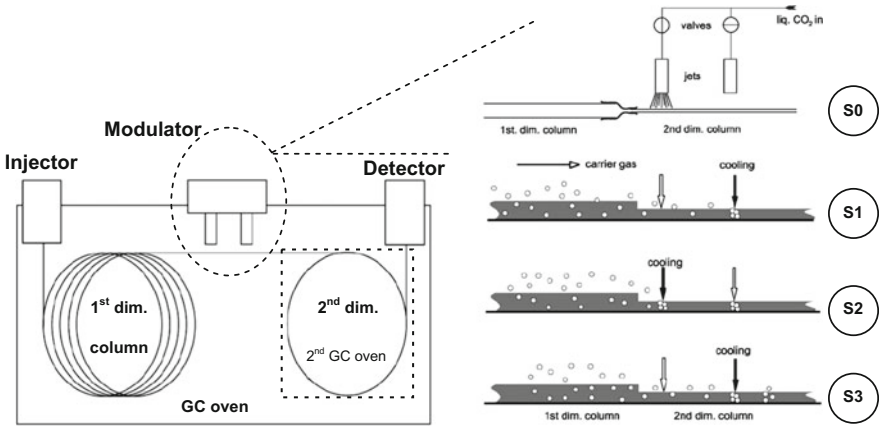

Fig. 13.3 (*Top left*) Schematic set-up of a GC×GC system, with optional second-dimension oven. (*Top right*) Schematic of dual-jet cryogenic modulator (S0), and modulator action: (S1) right-hand-side jet traps analytes eluting from first-dimension column; (S2) right-hand-side jet switched off, cold spot heats up rapidly and analyte pulse is released into second column; simultaneously, left-hand-side jet switched on to prevent leakage of first-column material; (S3) next modulation cycle is started. (*Bottom*) Illustration of modulation procedure and visualization of chromatogram (cf. [86])

also features an interface called the *modulator*, whose key role will be explained below. One should add that, for a separation to be truly comprehensive, three essential demands have to be met (*cf.* [13]):

- All sample constituents have to be subjected to two separations in which their transportation mechanism depends on different factors (*cf.* above).
- Any two sample constituents separated in the first dimension should remain separated in the second dimension.
- The elution profiles from both columns have to be preserved.

Returning to the schematic of Fig. 13.3 (top left), in most GC×GC systems, the sample is first separated on a high-resolution capillary GC column—typically with dimensions of 15–30 m × 0.25–0.32 mm ID × 0.2–1 μm d_f—which contains a non-polar stationary phase. Stationary phases often used are 100 % dimethylpolysiloxane and 95/5 dimethyl/phenylenepolysiloxane. The eluate from the first-dimension column is collected by/in the modulator and periodically introduced into the second-dimension column as a large number of adjacent small fractions. In order to maintain the integrity of the first-dimension separation, these fractions should be no larger than roughly one-quarter of the peak width in the first dimension—or, in comprehensive parlance, 3–4 modulations should be made across each peak. Since peaks on high-resolution first-dimension columns typically have baseline widths of 5–30 s, modulation times—and, consequently, second-dimension run times (see below)—should be on the order of 2–8 s. Practical experience shows that in order to meet the modulation criterion, temperature programming in GC×GC has to be slower than in 1D-GC and typically occurs at a rate of 1–3 °C/min. In the

modulator, each individual eluate fraction is trapped, refocused, and, next, launched into the second-dimension column as a very short chromatographic pulse. While this fraction is being separated on this second column, the modulator collects the next fraction of eluate from the first-dimension column. The process of effluent collection and re-injection is repeated throughout the entire analysis.

As pointed out above, the separation mechanism of the second-dimension column has to differ from that of the first-dimension column. Moreover, the analysis time on this column should be essentially the same as the modulation period, i.e. some 2–8 s. Consequently, the second column has to be much shorter and narrower than the first one—typically 1–2 m × 0.1 mm ID × 0.1–0.2 μm d_f—and the stationary phase usually is of a (semi-)polar or shape-selective nature; wax-based phases, 65–50/35–50 dimethyl/phenylenepolysiloxanes, and cyclodextrin phases are typical examples. Because the separation on this column is extremely fast, the analyte peaks are very narrow, with widths of some 100–600 ms at the baseline. Such narrow peaks require fast detectors with a small internal volume and a short rise time in order to achieve a proper reconstruction of the (second-dimension) chromatograms—a topic that will be discussed below.

In principle, all analytes present in a specific first-dimension eluate fraction should be eluted from the second-dimension column during the modulation in which they were injected on that column. If second-dimension peaks have retention times that exceed the modulation time and consequently show up in a later modulation, they are said to display *wrap-around*. Since this phenomenon adversely affects the quality of GC×GC chromatograms and complicates their interpretation, proper adjustment of second-dimension retention times is highly relevant. This is one reason why rather thin-film stationary phases are used in the second dimension. It also explains why some GC×GC set-ups feature a separate oven for the second-dimension column, viz. to enable more flexible and independent temperature regulation.

The raw GC×GC data that are collected at the detector are a continual stream of responses which are in effect a large series of short, high-speed second-dimension chromatograms, which are usually stacked side by side to form a 2D chromatogram, with one dimension representing the retention on the first column and the other, the retention time on the second column. A highly convenient way to visualize these chromatograms is as contour plots, with the peaks being displayed as spots in a 2D plane using colour, shading, or contour lines, or as 3D plots, to indicate signal intensities (Fig. 13.3). Alternatives are apex plots (simplified 2D plots in which peak apices are indicated only), and bubble plots where peak apices are indicated by bubbles and their areas represent the peak areas.

Modulation The modulator joins the first- and second-dimension columns and is a key component of the GC×GC instrument. Over the years much effort has been devoted to design and construct robust and user-friendly devices (see, e.g., [14–16]). For a recent review which extensively discusses the use of pneumatic modulators, the reader should consult [17]. Here, we will discuss only the most essential aspects. The modulator serves three main goals:

– Collecting and focusing each fraction eluting from the first-dimension column
– Re-injecting/launching each collected fraction into the second-dimension column
– Trapping the next first-column eluent fraction during the launch of the preceding fraction

Initially, heating was the preferred modulation principle, with a rotating slotted heater rapidly moving over a thick-film modulation capillary, heating it locally. Such a *sweeper* was frequently used in the early years of GC×GC, but because of the vulnerability of the set-up, the time-consuming optimization and the restricted (temperature-dependent) application range, it became obsolete in the late 1990s. Today, cooling is used almost exclusively to create the required retention/release temperature differences. The first cryogenic modulator was the longitudinal modulating cryogenic system which used expanding liquid carbon dioxide to trap the analytes at the top of the second-dimension column. By subsequently moving the trap rapidly to an upstream position, the refocused zone is exposed to the GC oven air and instantaneously volatilized and launched. Nowadays, jet-based modulators—which have no moving parts at all—with either carbon dioxide or liquid nitrogen for cooling are generally preferred; both single-, dual-, and quad-jet modulators have been introduced (Fig. 13.3, top right). The general experience is that all cryogenic modulators, if properly optimized, can satisfactorily be used for most applications, with a dual-jet modulator with carbon dioxide cooling probably being the best choice. Special attention is required only when very volatile compounds (boiling points lower than hexane) have to be determined. In such cases, cooling with liquid or cold gaseous nitrogen has to be used. Alternatively, valve-based modulation can be applied; however, this has not become very popular.

Column combinations In most studies, a non-polar stationary phase is used in the first-dimension column. This has the advantage that much information is available in the literature on the behaviour of a huge number of compounds on non-polar columns in 1D-GC which can be used to optimize the first-dimension separation. Here, volatility is the only parameter of interest, and, consequently, a boiling point separation is obtained. With all other types of column, separation will be primarily governed by the specific interactions of the selected (semi-)polar or shape-selective column but, to some degree, also by volatility. With a non-polar first column, in each individual, modulated fraction analytes with closely similar volatilities will elute from that column. Because of the fast and, thus, essentially isothermal second-dimension separation, for such analytes of equal volatility there will be no boiling point contribution in that dimension: only the specific interactions will govern analyte retention. In other words, the two dimensions operate statistically independently: the separation is therefore *orthogonal* and the entire 2D plane of the GC×GC chromatogram, the separation space, is available for peak separation [18, 19]. One main benefit of orthogonal separations is that *ordered structures*—i.e. continuous bands or clusters—now show up in most GC×GC chromatograms for structurally related homologues, congeners, and isomers [20, 21]. This is because chemically related compounds have similar functionality and, hence,

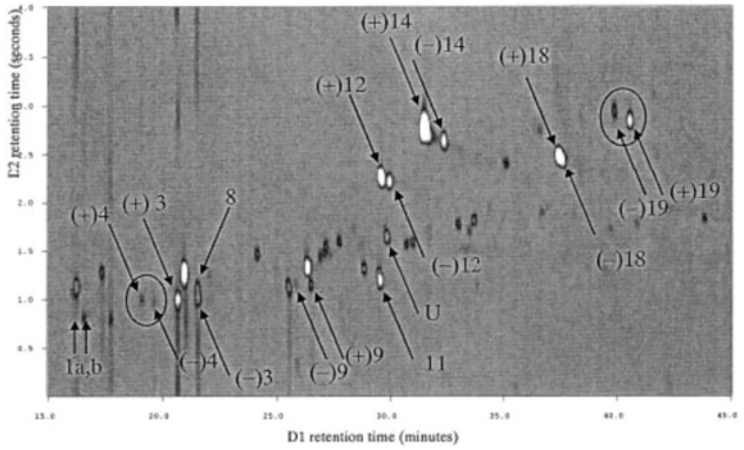

Fig. 13.4 Enantio-GC×GC–FID of a high pH distillation of a flush growth sample of tea tree essential oil. Peak numbers: (1) *α*-thujene, (3) sabinene, (4) β-pinene, (8) *p*-cymene, (9) limonene, (11) γ-terpinene, (12) *trans*-sabinene hydrate, (14) *cis*-sabinene hydrate, (18) terpinen-4-ol, (19) - α-terpineol, *U* unidentified component. Individual isomers indicated by (+) or (−) sign or a, b where correct assignment of isomers was not confirmed [25]

polarity: the 2D plane defines a type of chemical property map, determined by the choice of the stationary phases in the two GC columns. Structured chromatograms are a valuable tool when performing group-type identification and can also greatly aid in the identification of unknowns, as will be demonstrated in Sect. 13.3 (see, e.g., Figs. 13.5, 13.7, 13.8 and 13.13).

Despite the advantages of non-polar × (semi-)polar separations, there are also benefits in using so-called reversed-type column combinations. The most important advantages are gained for polar and/or ionogenic compounds. Polar alcohols and, specifically, carboxylic acids can often hardly been recognized if a conventional column set is used. However, with a reversed set-up, peak shapes are fully satisfactory and there also are ordered structures (see Sect. 13.3.1). Other examples include the determination of pyrazines in coffee beans [22], of flavours in food extracts [23], and of amino acids in wine, beer, and honey [24]. Obviously, in such instances, the contribution of analyte volatility to the first-dimension separation is negligible and orthogonality can therefore be achieved also here.

Reversed-type column combinations are also used in enantiomeric analysis. The separation of enantiomeric pairs on an enantioselective—usually a cyclodextrin-type—phase requires long run times to obtain sufficient resolution. The reversed-type approach is therefore preferred if ordered structures are not of interest. A conventional column combination gives better results if 'structure' is required, but the analysis is more demanding (e.g. the use of vacuum outlet conditions) because enantiomeric resolution now has to be effected during the fast second-dimension separation. Examples of the use of both achiral × chiral and chiral × achiral strategies include the analysis of terpenes in tea tree essential oil (Fig. 13.4) [25]), of

volatile oils in traditional Chinese medicines, of flavours in wine and strawberry volatiles [26–28], and of chiral CBs in grey seals, milk, cheese, and salmon [29–31]. In several instances, enantio-enrichment was observed [32].

An aspect that is not often addressed in the literature is the optimization of the column combinations in terms of the stationary phases selected. The practical relevance of such optimization was demonstrated by Korytár et al. [33, 34] in studies on, e.g., between- and within-class separations of many different classes of organohalogens on a series of non-polar × semi-polar column sets. System optimization for specific applications has also been performed, e.g., by systematically changing the first-dimension stationary-phase conditions to separate critical pairs [35] or by using GC×2GC with two second-dimension columns of widely different polarities (and a split of the first-column effluent). In one application, with dual FID detection, over 100 volatiles present in air/breath were separated within 10 min [36]. It has also been recommended to use a twin system, which allows the simultaneous analysis of a sample on two mutually different and independent column combinations (e.g. a conventional and a reversed one) housed in the same oven, i.e. under identical conditions [23, 37]. The determination of FAMEs in olive oil and that of linear alkylbenzenes in sediment are reported as applications [38].

Temperature programmes of GC×GC separations usually are made rather slow to meet the modulation criterion (*cf.* above). Obviously, it is of interest to decrease run times by optimizing the GC column dimensions. The use of a relatively short and small-bore second-dimension column has been found to cause an up to fourfold reduction of the time of analysis [39]. More importantly, models have been devised that allow the calculation of optimum gas pressures and flow rates in a GC×GC system [40–42]. One conclusion was that one column should be operated close to its optimum flow conditions, and a sub-optimum separation of the other column accepted.

13.2.2 Detection

Since its introduction, GC×GC has been combined with some ten types of detector (see, e.g., [23] and [43]). From among these, three types are in vogue today:

- The flame-ionization detector (FID), particularly for group-type petrochemical applications and for general developmental studies
- The micro electron-capture detector (μECD), almost exclusively for the organohalogen field
- Most importantly, time-of-flight and, less frequently, rapid-scanning quadrupole mass spectrometers (ToF MS and qMS, respectively), for all applications in which identification and/or identity confirmation play a role

FID and element-selective detection As was discussed above, the widths of peaks eluting from a second-dimension column are 100–600 ms and the rise time of the detector should, therefore, be short and its internal volume small. Theory as well as

experimental evidence shows that for the proper quantitative description of a peak, the acquisition rate of the signal should be at least 100 Hz. In the early years of GC×GC, detection had therefore to be performed with an FID: modern FIDs have a negligible internal volume and can acquire data at frequencies of 50–300 Hz. In the early 1990s, the dominating role of the FID did not create real problems, since most studies were devoted to system optimization and general performance testing. Moreover, most early applications were in the petrochemical field where PIONA-type determination of sample composition is important, and the FID is the detector of choice. FID detection is popular also because of the excellent (*C*-based) analyte detectability and the long dynamic range of some five orders of magnitude.

In the late 1990s, when trace-level detection and, specifically, the detection of organohalogens rapidly gained interest, several miniaturized electron-capture detectors were marketed. The Agilent (Palo Alto, CA, USA) micro-ECD (μECD) with its small, i.e. 150 μl, internal volume and an acquisition rate of 50 Hz, was found to yield satisfactory results [15] and is widely used also today. Optimum performance requires high detector temperatures (320–350 °C) and high auxiliary gas flow rates (150–450 ml/min). With GC×GC–μECD, very low limits of detection (LODs) can be obtained for halogenated micro-contaminants, e.g. 50–150 fg for all priority CDD/Fs [44].

For the use, in GC×GC, of other element-selective detectors such as, e.g., the *S*-selective and *N*-selective chemiluminescence detectors, a (conventional) *N*/*P* detector, and, even, an atomic emission detector, the reader should consult the quoted literature [45–51].

Mass spectrometric detection Element-selective detectors permit more or less selective peak recognition, but they do not provide structural information. If such information is required to enable unambiguous identification or confirmation of identity, and/or to ensure high selectivity throughout a chromatogram—and this is increasingly true today—a mass spectrometer (MS) has to be used. This is convincingly demonstrated by the well-known high popularity of conventional GC–MS, and also by the rapidly increasing number of GC×GC–MS-based studies (see below).

ToF MS detection In the early days of GC×GC, no commercial MS detector could cope with that overridingly important aspect of the technique, a sufficiently high data acquisition rate. Fortunately, in the early 1990s a ToF MS instrument was marketed by Leco (St. Joseph, MI, USA) that provided, at unit-mass resolution, a very high acquisition range of some 100–500 spectra/s. With such acquisition rates, proper reconstruction of even the most rapid second-dimension peaks does not present any problems, and neither does the subsequent deconvolution of overlapping peaks or peak quantification. The successors to the first commercial instrument, the Pegasus II, are the Pegasus III and, recently, the Pegasus IV, completely integrated instruments with advanced tuning and software facilities [52, 53]. For several classes of organohalogens—notably the polychlorinated alkanes (PCAs) and polybrominated diphenyl ethers (PBDEs) [52]—EI-MS causes too much fragmentation to provide meaningful structural information and a soft

chemical ionization mode such as electron-capture ionization (ECNI) has to be used instead. To quote an example, GC×GC–ECNI-ToF MS with a Thermo Electron (Austin, TX, USA) instrument was successfully applied to interpret the ordered structures observed for PCA mixtures [54] (see Sect. 13.3.3), to PCBs in bovine fat [55], and to characterize fatty alcohol alkoxylate polymers up to 700 Da [56]. In the last-named study block and random co-polymerization could be distinguished and the starter building block within a block copolymer group identified.

From the very beginning it was clear that the principal blessings of the new technique—the generation of a huge amount of high-quality data—also created a main stumbling block: instead of the GC×GC run itself, data handling now became the real and refractory problem. Dallüge et al. [57–59], who used a Pegasus II system, discussed the potential and limitations of GC×GC–ToF MS data processing and the strategies for solving a variety of application-orientated problems. Figure 13.12 (see Sect. 13.3.4) illustrates their approach which, implicitly or explicitly, was also used by many other workers. The scheme provides the newcomer to the field with a good general idea of the process. With the newer generation systems such as, e.g., the Pegasus III and IV with their Leco ChromaToF™ software, a distinct step forward has been made and, with partial automation instead of manual operation, the operator's task has been alleviated considerably. Because of the commercial nature of the software, no detailed discussion can be given. It is probably true to say that most applications aimed at the detection/identity confirmation of even large numbers of *target compounds* now are fairly straightforward. However, if *unknowns* are the main issue—as in, e.g., many air analyses and metabolomics, and in quite a number of organohalogen and essential oil studies—automated detection and data presentation still are complex and time-consuming operations. In-depth discussions, and partial solutions, of these problems can be found in several papers published by Zimmermann and his group [54, 60, 61].

For a wide ranging selection of studies applying ToF MS detection, the reader should consult Tables 13.1, 13.2, 13.3, 13.4, and 13.5 below.

qMS detection Because of the high price of a ToF MS instrument, and also because of the expertise required to handle the generated data, several groups of workers have studied the potential of GC×GC combined with a state-of-the-art qMS. Such studies convincingly demonstrate that, generally speaking, this technique does not provide satisfactory results at all unless a seriously restricted mass range—or, even better, selected/single-ion monitoring—is used. Under such conditions, it will be possible to successfully perform a variety of not too demanding target analyses using the SIM [62] and even the TIC [39] mode.

Some years ago, rapid-scanning qMS instruments were introduced, such as the Shimadzu (Milan, Italy) QP2010, the Perkin-Elmer (Shelton, CT, USA) Clarus 500, and the Thermo Electron (Waltham, MA, USA) Trace DSQ, which were immediately found to be distinctly superior to conventional machines [44, 63–67]. Two examples are quoted here. For a mass range of 200 Da, an acquisition rate of 33 Hz was achieved, which corresponded with a minimum number of 7–8 data points across a peak for several classes of compounds [64]. In the time-scheduled

mode (50–100 Da mass windows to cover a wide mass range in a single run) the mass spectra from the seven windows required to cover the *m*/*z* 188–494 mass range of all PCBs and obtained at 33–50 Hz contained sufficient information to correctly identify the congeners of interest. In another paper [44], GC×GC–ECNI-rapid-scanning qMS was used to study several classes of organochlorines and chlorobornanes. Resolution and mass spectral quality were satisfactory up to 9,000 Da/s, but quantification close to that level was less precise. LODs of 10–40 fg were found for ten out of eleven PBDEs and of 10–110 fg for 15 out of 17 priority PCDD/Fs (unfortunately, the key compound, 2,3,7,8-TCDD, had a 'high' LOD). More recent studies confirm the practicality of rapid-scanning qMS detection, using, e.g., the Shimadzu QP2010 Plus [68], the Trace DSQ [69–71], or the Agilent (Palo Alto, CA, USA) HP 5975B [72, 73]. With the Varian (recently purchased by Agilent) 1200-1, next to the pulsed flow modulator, a main feature is the combination of GC×GC and triple-quadrupole qMS via a supersonic molecular beam interface [74]. To quote an example of real-life application, Schmarr et al. used the Trace DSQ to detect volatiles in fruits [69] and red wine [71], and alkylmethyl-oxypyrazines in grape must and wine [75].

HRMS detection Very powerful but also highly expensive and labour-intensive HRMS detection has been combined with GC×GC in a few studies. In one case, HRMS as well as NPD and qMS detection were used to characterize atmospheric nanoparticles [76]. PCDD/Fs in crude extracts of fly ash and flue gas were quantified using a JEOL (Akishima, Tokyo, Japan) JMS-T100 GC [77], and dioxins were determined in human serum with LODs at the attogram level (S/N of 400:1 for 313 ag of 2,3,7,8-TCDD) [78].

In summary, for the many applications with a limited mass range of, say, 100–300 Da, a rapid-scanning qMS is a useful alternative to a ToF MS. However, whenever target analyses cover a wide mass range or are distributed such that time scheduling does not offer a solution and, of course, whenever searching for unknowns is a key aspect of a study, using a ToF MS instrument becomes necessary.

Analyte detectability In the early years of GC×GC, several authors reported a 10–70-fold increase in analyte detectability—i.e. a corresponding decrease of LODs—when replacing 1D-GC by the comprehensive technique. However, more recent studies show that such results were not obtained under conditions which were optimized for both techniques. Both theoretical and experimental (μECD and ToF MS) evidence indicates a modest 2–5-fold improved sensitivity for GC×GC, with refocusing in the modulator probably being the main cause of the beneficial effect [21, 57, 79, 80].

For the rest, the reader should always keep in mind that in experimental practice, i.e. when analysing (highly) complex samples, analyte detectability is often limited by the presence of a high and noisy background generated by co-eluting sample constituents. Due to the much improved resolution of GC×GC as compared with 1D-GC, such interferences are often efficiently separated from the analytes of interest. Consequently, analyte detectability is now frequently enhanced to a much higher degree than can be derived from the formal presentation given above.

Finally, in the early years of GC×GC there was a feeling that quantification would probably be less satisfactory than in conventional 1D-GC. However, selected experimental results included in two early reviews show convincingly that analytical performance data for both techniques are closely similar [79, 81].

Chemometrics Here, it would be appropriate also to discuss the use of chemometric and other related techniques for all aspects of data analysis. However, because of the rather complicated nature of the subject matter—which is, moreover, to our opinion not of primary importance in an introductory and application-orientated text—we prefer not to include this topic in the present text. Instead, we refer the interested reader to extensive discussions and/or lists of references included in review papers such as [79] and the more recent [82], and Chapters 4 (Data acquisition, visualization and analysis; by Reichenbach [83]) and 5 (Chemometric approaches; by Hoggard and Synovec [84]) in the Ramos textbook [85].

13.3 Applications

Since its introduction in the early 1990s, over 500 papers on GC×GC have been published. A large majority of these are application orientated. Three relatively recent review papers (with, each, hundreds of references) are available [43, 86, 87]. A much more detailed study of the merits of the comprehensive GC approach and its huge practical potential can be found in an excellent multi-author book [85]. In the present section, we discuss a limited number of studies selected in order to illustrate the various types of compound class and sample type that have been subjected to GC×GC analysis—and, even more so, to illustrate the types of 1D-GC and GC–MS problems that can be solved successfully by using the comprehensive approach. Most of this set of examples is taken from the somewhat older literature—mainly because in early studies relatively much attention was devoted to demonstrating the high potential of the novel approach. In addition, these studies frequently provide interesting information on the development, and application, of optimization strategies. In order to present a wider ranging overview of the practical usefulness—and, specifically, the state of the art—of GC×GC today, Tables 13.1, 13.2, 13.3, 13.4, and 13.5 list a variety of selected applications, with emphasis on more recently published papers.

13.3.1 Food, Fat, Oils, Flavours, and Fragrances

A number of key studies published in the food, fat, and flavours area is briefly discussed below. A selection of recently published papers is included in Table 13.1 [154–170].

Table 13.1 Selected papers on GC×GC of food, fat, oils, and fragrances

Area of application	Detection	Ref.
C18:1 isomers in milk fat and beef fat	FID	[154]
Honey volatiles (e.g. for traceability studies)	ToF MS	[155–157]
Olive oil volatiles: traceability, pattern recognition	ToF MS	[158, 159]
Volatile nitrosamines in meat products	NCD	[160]
Volatiles in Brazilian cachaça: analysis and fingerprinting	ToF MS	[161–163]
Benzenic and halogenated volatiles in animal-derived food products	ToF MS	[164]
Substituted pyrazines and other volatile aromatics in potato chips	ToF MS	[165]
Roasted food matrices: coffee, hazelnut, barley	FID, qMS, ToF MS	[166–168]
Volatile oil composition of *Eucalyptus dunnii*	qMS, ToF MS	[169]
Odour-active compounds in spicy fraction of hop essential oil	ToF MS	[170]

Fats and oils Fatty acids (FA) are almost invariably analysed by means of 1D-GC after their transesterification hydrogenation to methyl esters (FAMEs). For complex samples, adsorption LC is sometimes used to effect a fractionation prior to GC analysis. When minor FAs eluting close to much more abundant homologues are of interest, more selective MDGC is frequently used.

Early studies [20, 81, 88] showed that, in non-polar × polar GC×GC, FAMEs with the same number of carbon atoms elute as clusters, with a gradual increase of the first-dimension retention times with increasing carbon number, while second-dimension retention times increase with an increasing number of double bonds (saturates to hexa-unsaturated). An illustrative example is shown in Fig. 13.5a [20], with results for C16:0 through to C22:0 FAs, as their FAMEs, in herring oil [81]. The quoted papers convincingly demonstrate that one main advantage of the improved resolution of GC×GC is that odd-numbered isomers—which are often present as minor constituents—can now be recognized easily.

Mondello et al. [89] preferred GC×GC to characterize FAMEs in cod liver oil because FAME differentiation by GC–MS is difficult as many esters are characterized by similar fragmentation patterns. The ultra-trace-amount compounds, especially in the C15, C17, C19, C21 FAME groups, were clearly visible in the 2D plane. Alignments similar to those quoted above were observed, within each FAME class, for esters with the same number of double bonds, and for FAMEs with the same ω number. Figure 13.5b [89] shows, for the C20 FAMEs, how these patterns can be exploited, via their intersection points, for reliable peak assignment.

GC×GC–ToF MS has been used also to characterize known and unknown compounds from various classes of lipids such as FAs, fatty alcohols (FALs), diols, sterols, and hydroxyl acids (Hy-As) in lanolin [90], with methylation plus silylation as the preferred route to obtain high-quality chromatographic separation of the compound classes of interest. The dual derivatization caused a sharp decrease of the polarities of the FALs, diols, and Hy-As: their log *P* values increased by 3–4 logarithmic units. Easily recognizable ordered structures were observed.

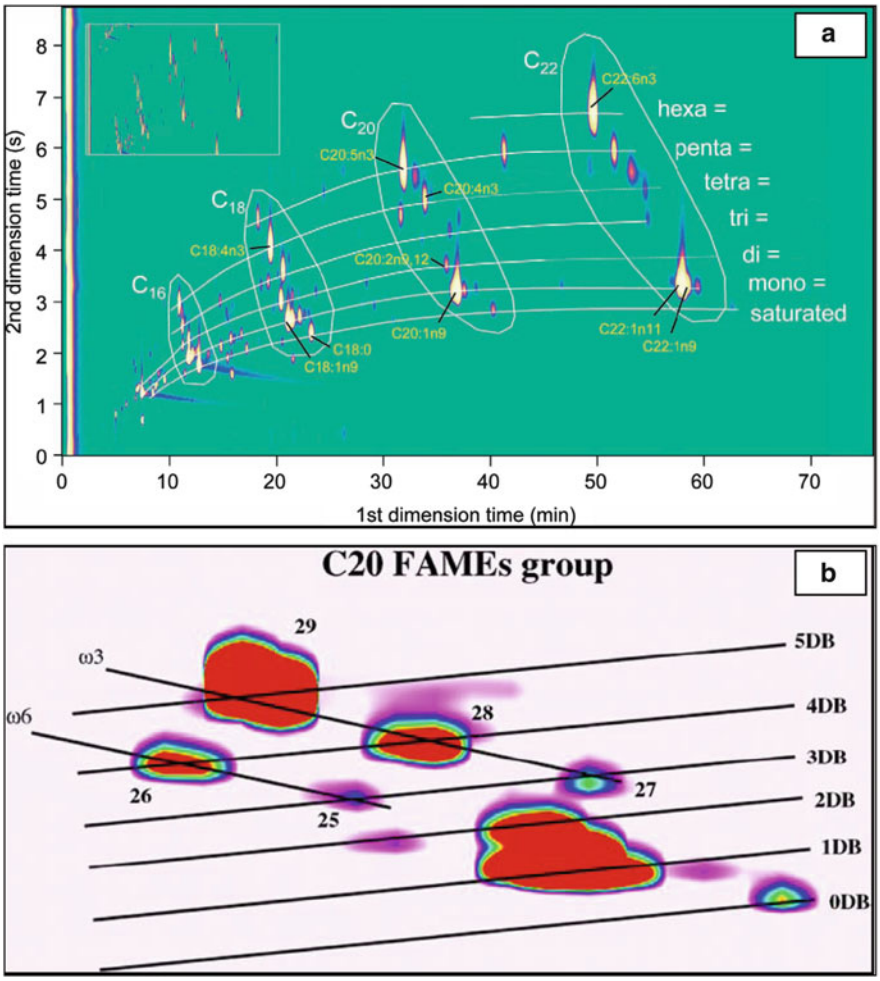

Fig. 13.5 (**a**) GC×GC–FID of herring oil on HP-13 × CP-Wax-52. *Lines* indicate fatty acids with same number of double bonds (DB), and polygons fatty acids with same number of carbon atoms. The original 2D plot (*insert*) was modified to avoid wrap-around [20]. (**b**) Expansion of chromatogram of cod liver oil FAMEs (C20 group). Peak identification: (25) C20:3ω6; (26) C20:4ω6; (27) C20:3ω3; (28) C20:4ω3; (29) C20:5ω3 [89]

Separation of *cis*/*trans* FAME isomers was achieved on CP-WAX × VF-23ms [91]. The WAX column creates separation in terms of FAME chain length and the number and position(s) of the double bonds. The 3-m long (!) VF-23 ms column efficiently separated the *cis*/*trans* isomers at a constant temperature of 165 °C. This approach should improve the reliability of the quantification of the *trans* isomers. The same group of authors compared the performance of one- and (comprehensive) multidimensional chromatographic systems for the characterization of triacylglycerides (TAGs) in edible oils and fats. $GC_{FAME} \times GC_{FAME}$ was

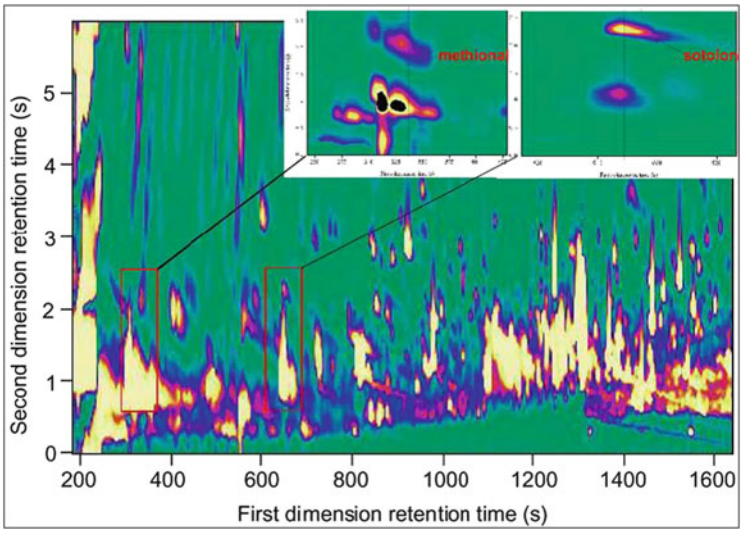

Fig. 13.6 Total ion current plot of GC×GC–ToF MS of a brunch extract. *Inserts*: (*left*) methional with extracted-ion trace *m*/*z* 104; (*right*) sotolon with extracted-ion trace *m*/*z* 128. In both instances, target analytes are 'highest' spot on *vertical line* [92]

found to provide all the information required in the daily routine analysis of fat samples in about 2 h. Admittedly, $AgLC_{TAG}\times GC_{FAME}\times GC_{FAME}$ analysis of a complex TAG (with online derivatization after the first dimension) is more powerful, but this typically requires 36 AgLC fractions each to be subjected to an approx. 2 h $GC_{FAME}\times GC_{FAME}$ run. That is, the total analysis time now is some 3 days!

In the trace analysis of flavour compounds in food, their separation from interfering matrix constituents is an aspect of much interest. In one study [92], methional and sotolon had to be separated from a complex dairy spread extract. In the first dimension, both analytes co-eluted with major peaks, 2-heptanone and 2-nonanone, respectively (Fig. 13.6). 1D-GC–MS cannot solve this problem because *m*/*z* 104 (methional) and *m*/*z* 128 (sotolon) are abundantly present in the co-eluting background (see inserts). However, with the comprehensive approach, clear mass spectra were obtained for both target analytes and quantification at the 40–90 ng/g level was straightforward. In the same paper, rewarding separations and ordered structures were found for δ- and γ-lactones, aldehydes, alcohols, ketones, and acids, using a CP-Sil 5 CB × BX-50 column combination. For the C_{14}–C_{18} acids, the beneficial role of GC×GC in eliminating the adverse effect of tailing on the detection of minor constituents in 1D-GC was highlighted.

A much more beneficial effect of using the reverse BP21 × BPX-35 set-up was observed when analysing flavours in vanilla extracts and olive oil [23]. For most polar analytes that had to be studied, aldehydes, 2-enals, alcohols, and dienals, the conventional approach provided ordered structures—but not for the carboxylic acids nor for some alcohols. Specifically, with the acids, the individual compounds could not be recognized because of their high retention on the second-dimension

column, which caused serious peak broadening and wrap-around. Switching to the reverse set-up effected a marked improvement. The peak shapes of all target analytes were now fully satisfactory, and ordered structures showed up. Similar observations were made for butter samples [93]. Here, special attention was paid to selective ToF MS of C_6–C_{16} δ-lactones and odd- and even-numbered C_5–C_{12} carboxylic acids. The MS match factors were much higher for GC×GC than for 1D-GC.

Allergens in consumer products are an important concern for the EU with, e.g., 26 substances having to be indicated on the labelling if they are present in concentrations exceeding 0.001 % in cosmetics intended to remain on the skin. Routine GC–MS can be used to analyse 24 out of these 26 allergens in consumer (and intermediate) products, but insufficient peak capacity and peak-shifting easily cause problems. On the other hand, GC×GC on SPB-1 × SupelcoWax-10 yields a satisfactory separation of all 24 allergens in a mere 30 min [94]. A baseline separation was effected for the often occurring α- and β-ionone from each other and from trace-level α-isomethylionone. Quantification of the target allergens (specifically the difficult linalool and anisyl alcohol) using qMS in the SIM mode (detection frequency, *ca*. 30 Hz) was successful, even with a HP 5972 [62].

The SIM-mode approach is, of course, only suitable for target analysis. The use of a rapid-scanning qMS eliminates this problem for a wide variety of complex samples [64, 66, 95]. For example, when a mass range of up to 200 Da was monitored at an acquisition frequency of 33 Hz, identification and quantification of flavour compounds in olive oil and allergens in fragrances posed no problems, with LODs down to 2–10 pg.

A combination of GC–MS and GC–olfactometry (GC–OLF) is often used to analyse complex perfume samples. Assessment of odour-active components is based on the correlation between peaks of eluted substances perceived simultaneously by the MS and the human olfactory system. However, co-elutions may mask odour-active trace analytes by major interferences or an agglomeration of olfactive impressions. Applying GC×GC–OLF is a powerful alternative. In one study 481 out of 818 compounds presented odour activity through GC×GC–OLF as against 135 out of 177 through GC–OLF [96]. GC×GC–qMS was used for compound identification.

Essential oils are moderately to highly complex samples comprising a wide range of classes of compounds and very long capillary GC columns are therefore used in 1D-GC to achieve adequate resolution. Today, GC×GC on both conventional and reversed column sets is preferred, with ToF MS detection for reliable identification of the detected compounds. Examples include the analysis of essential oils from the hulks of pistachio nuts extracted by direct thermal desorption (DTD) [97], from coriander leaves and hops via combined GC–OLF and GC×GC–ToF MS [98], and from tobacco leaves [99]. In these papers, and also in studies on zedoary [100, 101] essential oils and volatile oils in traditional Chinese medicines [26], it is the huge numbers of compounds detected and reliably identified that attracts most attention. One study on hop essential oils [102], 1,000–1,500 peaks with $S/N > 25$ showed up; 119 components could be reliably identified and, out of

these, no less than 45 for the first time. With the Chinese medicines, an unusually powerful 60 m × 3 m long column set was needed to achieve adequate separation: 800 separated peaks—as against a mere 80 in 1D-GC—were observed. Some 50 % of these were identified by ToF MS, e.g. some 100 ketones, over 80 alcohols and hydrocarbons, close to 40 aldehydes and 20–30 of each ethers, esters, and acids [26].

DTD–GC×GC–ToF MS has been applied to study the extraction of essential oils from nuts (*cf.* above), to directly quantify volatiles from leaves [103] and to examine the effect of maturation on the composition of Cheddar cheese volatiles [98]. This suggests that the online technique can be used advantageously in controlling production processes.

Miscellaneous food samples Other types of application in the food area include the analysis of the volatile fraction of roasted coffee beans on a polar × non-polar column set, selected because of the many polar analytes expected to be present. About 1,000 separated analytes showed up in the 2D separation space as against only about 200 in conventional GC–MS. Notable differences were observed between Robusta and Arabica volatiles [22]. In a study on the headspaces of various types of pepper samples, in a Brazilian pepper over 700 compounds were identified by GC×GC–ToF MS (most of them in trace amounts) as against only some 140 when using GC×GC–qMS—a clear example of the superiority of the time-of-flight instrument [104]. A combined GC×GC–ToF MS plus GC–OLF strategy was shown to be markedly successful in the detection and identification of up to 100 *S*-containing compounds—e.g. thiols, sulphides, thiophenes, and thiazoles—in roast beef aroma [105].

13.3.2 Biological/Biota Samples

Several relevant studies on the analysis of bio-type samples are discussed below. Table 13.2 lists selected recent papers dealing with this subject matter [73, 171–179].

A multibed sorption trap combined with GC×GC–ToF MS [106] or GC×GC–FID [107] was used to analyse VOCs in human breath. This is a minimally invasive medical diagnostic method and can also be used to monitor human exposure to environmental toxins. Some 250 compounds were detected in the samples, and 60 % of these could be identified. One application was trying to find suitable breath biomarkers for active smoking. 2,5-Dimethylfuran together with two new compounds (2-methylfuran and furan) appeared to be promising candidate for breath biomarkers as they are found in breath more than 2 h after smoking.

In the field of metabolomics, characterizing a diversity of biological systems in terms of their overall metabolite profiles is an important aspect, with biomarker discovery as the final goal. When spleen samples of obese mice and lean control strains were analyzed after derivatization with *N*-methyl-*N*-trimethylsilyltrifluoroacetamide (MSTFA), comparison of GC×GC–ToF MS and 1D-GC–ToF MS

Table 13.2 Selected papers on GC×GC of biological/biota samples

Area of application	Detection	Ref.
Metabolic profiling of infant urine: diagnosis of organic acidurias, biomarker discovery	ToF MS	[171]
Anabolic agents in doping control	FID, ToF MS	[172]
Fluoride-induced regenerated nerve agent in biological samples	ToF MS	[173]
Bacterial fatty acids	FID/qMS	[73]
Micro-pyrolysis of technical lignins	FID, ToF MS	[174]
Biomarker discovery for diabetes mellitus	ToF MS	[175]
Hydroxylated PAHs in urine	FID	[176]
Characterization of polar biopolymers	ToF MS	[177]
Studies of drug-induced liver injury	ToF MS	[178]
Metabolic phenotyping of natural variants in rice	ToF MS	[179]

showed a sevenfold increase of the number of hits (with S/N > 50). In addition, the purity of the mass spectra was much improved. Several potential obesity biomarkers were tentatively identified, with sugar alcohols and unidentified compounds appearing to be more important than the (expected) free fatty acids, glucose, or cholesterol [108]. Since, in such studies, biological variability exceeds the analytical error, a fairly large number of biological replicates have to be analysed. Consequently, high-throughput analyses are required and, also, automated statistical procedures to evaluate and compare the resulting chromatograms. These problems were addressed, and partly solved, in a subsequent paper [109].

GC×GC–ToF MS was also used to detect and quantify metabolite differences between yeast cells growing in different media; over 20 metabolites were identified which differentiate repressed from de-repressed cells [110]. In a study on chemical differences of (TMS-derivatized) metabolites in plant samples [111], a PCA-based method was used as a first step to automatedly compare such complex chromatograms and locate metabolites that significantly differ between species. Basil, peppermint, and sweet herb stevia were differentiated successfully, with the relative abundances of amino acids, carboxylic acids, and carbohydrates being responsible for this differentiation.

Combined strategies can help to solve particularly refractory problems. GC–EAD (electroantennographic detection) and GC×GC–ToF MS were used to analyse a female sex pheromone gland extract of the persimmon bark borer, *Euzophera batangensis*. GC–EAD produced responses in two areas where no compounds were detected by GC–FID, while GC–MS did not provide any relevant mass spectra to enable identity confirmation, since the MS signal was hidden in the background noise. However, GC×GC–ToF MS of the problem area indicated the presence of, among others, (9*Z*, 12*E*)-tetradeca-9,12-dien-1-ol and (9*Z*)-tetradec-9-en-1-ol, which are pheromone components of closely related *Euzophera* species. The comprehensive separation was especially useful for the clear separation of a substantial 'wall' of chemical noise (column bleed, traces of solvent, etc.) from the analytes of interest. The two quoted analytes may be considered candidates for female sex pheromone components in *E. batangensis* [112].

13.3.3 Organohalogen Compounds

Real progress in the field of GC×GC analysis of organohalogen compounds had to await the introduction of the miniaturized Agilent μECD (*cf.* above). LODs as low as 6–20 fg of injected mass were then reported for individual CBs and CDD/Fs [113] and 30–150 fg for seventeen 2,3,7,8-substituted CDD/Fs and 12 dioxin-like CBs [93]. Selected recent papers on organohalogen analysis are included in Table 13.3 [77, 115, 123, 180–186]. Further relevant information is presented below.

Aromatic organohalogens The creation, and use, of ordered structures is a most important aspect of the detection of aromatic organohalogens at the trace level, especially because of the highly complex composition of their technical mixtures. Korytár et al. [21] observed such structures for some 90 CBs on a HP-1 × HT-8 column set. The number of chlorine substituents and the *ortho* vs. non-*ortho* positions were the main parameters of interest (Fig. 13.7). The high second-dimension retention times of the non- and mono-*ortho* CBs will facilitate their determination in complex real-life samples. A complete separation of all 12 WHO CBs and the 17 priority CDD/Fs was obtained on several close-to-orthogonal column sets. From among these, DB-XLB × LC-50 was the preferred choice if separation from matrix (milk) constituents was taken into account. In a study on all 209 CB congeners [114], combining DB-XLB with a biscyanopropyl siloxane or a liquid crystal column effected the separation of some 180 congeners, and close to 130 (out of the 136) congeners present in Aroclors 1242, 1254, and 1260 at over 0.05 wt.%. As an application, 64 CB congeners were identified and quantified in the blubber of a female grey seal.

GC×GC–ToF MS was used for the successful separation, within 1 h, of the 17 priority CDD/Fs in the presence of potentially interfering co-planar dioxin-like CBs on a 60 m Rtx-Dioxin 2 × 2 m Rtx-PCB 8 column set [115]. With a quad-jet dual-stage modulator, the modulation time had to be 4 s or less in order to preserve the first-dimension GC separation of all the CDD/Fs. In the 50–90 eV EI range tested, 80 eV gave more efficient ionization than the standard 70 eV, without an apparent effect on the mass spectra.

Other workers used the same 60-m first-dimension column which yielded good resolution of the priority dioxins and furans (and non-*ortho* CBs) and has high thermal stability [116]. An Rtx-500 phase was preferred for the second dimension because of the clean separation of the target analytes from the bulk of the matrix (fish) interferences: many of these were biogenic material with masses similar to those of the analytes of interest. All target analytes were baseline separated except for one critical pair (2,3,7,8-TCDD, TEF 1.0, and the usually much more abundant CB 126, TEF 0.1). The problem was solved by using properly selected, i.e. non-shared, masses for detection. Figure 13.8a illustrates the separation obtained for the most critical congeners; Fig. 13.8b shows part of the hexa-CDD/F region of a fish-sample extract. The reconstructed 1D-GC chromatogram is included for comparison.

Table 13.3 Selected papers on GC×GC of organohalogen compounds

Area of application	Detection	Ref.
BDEs and their hydroxylated and methoxylated metabolites in environmental samples	HRMS	[180]
Quantitation of multiple classes of organohalogens in fish oils	ToF MS	[181]
209 CB congeners on efficient non-selective capillary column	qMS	[182]
Pathways for anaerobic microbial debromination of BDEs	μECD	[183]
Halogenated 1′-methyl-1,2′-bipyrroles in marine mammals	ToF MS	[184]
Screening of persistent organohalogens in environmental samples	μECD	[185]
CDD/Fs in crude extracts of fly ash and flue gas from municipal waste incinerators	HR-ToF MS	[77]
CDD/Fs in fish oil, food, and environmental samples	ToF MS	[115, 186]
Toxaphene enantiomers in commercial fish oil	μECD	[123]

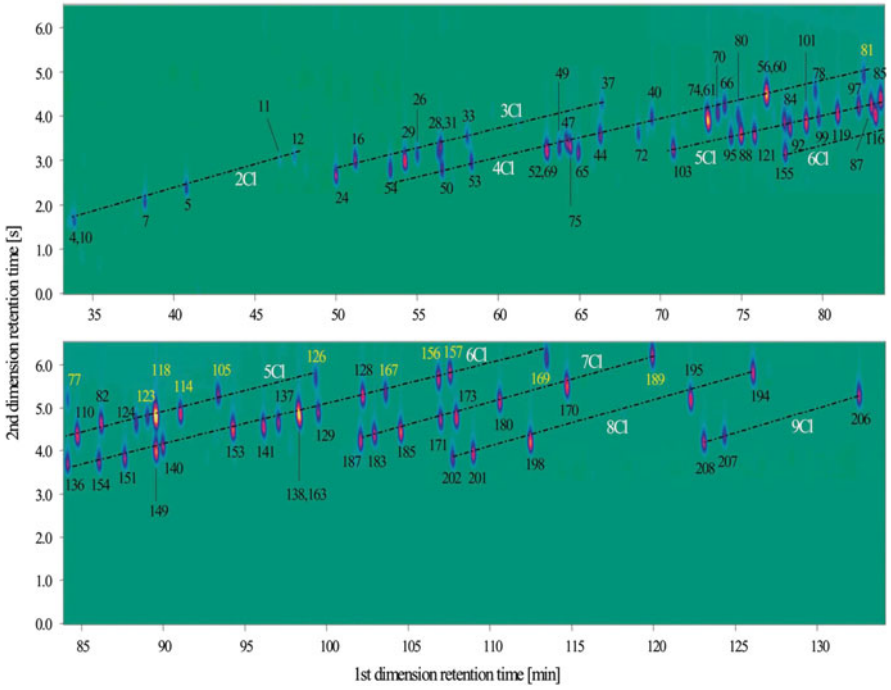

Fig. 13.7 GC×GC–μECD of a mixture of 90 CBs on HP-1 × HT-8 column set. *Colour codes* indicate number of chlorine substituents and principal non/mono-*ortho* congeners [21]

In a study of the priority CDD/Fs and WHO CBs in fish oil, cow milk, vegetable oil, and an eel extract, GC×GC–μECD was compared with 1D-GC–HRMS [117]. With a DB-XLB × LC-50 column set, the congener-specific and TEQ data agreed well with the reference values. The main conclusion was that GC×GC–μECD can become a powerful screening method for the determination of TEQs in food and feed. Improved sample clean-up will be needed for quantification.

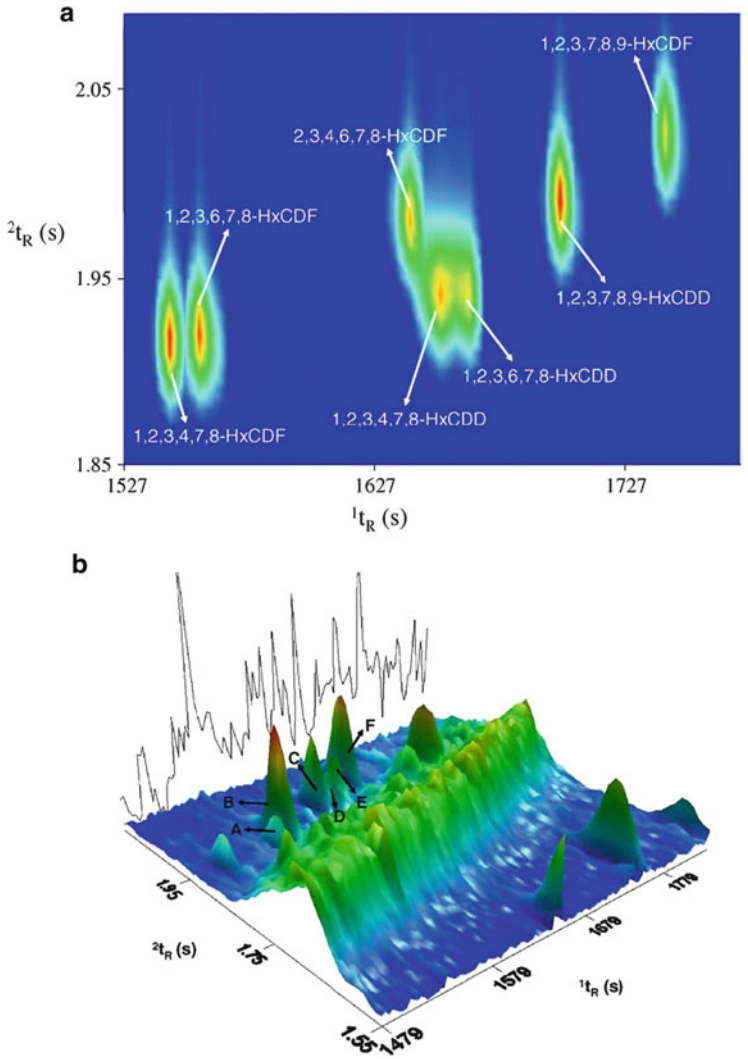

Fig. 13.8 (**a**) Part of GC×GC–ToF MS chromatogram of a standard solution containing 1 ng of HxCDD/Fs. Deconvoluted ion current (DIC) based on sum of molecular ions corresponding to HxCDD/Fs (*m/z* 390 + 374). (**b**) Part of HxCDD/F region of GC×GC shade surface plot after injection of clean-up fraction containing PCDD/Fs isolated from a fish sample; DIC: *m/z* 390 + 374. Concentrations, 2–3 ng/ml (A: 1,2,3,4,7,8-HxCDF; B: 1,2,3,7,8,9-HxCDF; C: 2,3,4,6,7,8-HxCDF; D: 1,2,3,4,7,8-HxCDD; E: 1,2,3,6,7,8-HxCDD; F: 1,2,3,7,8,9-HxCDD) [116]

In many studies on enantiomeric pairs of CBs, a 10–30 m Chirasil-Dex column was found to be the best choice in the first dimension (see e.g. [29–31]). Harju et al. [31] studied nine atropisomeric CB pairs, and the WHO non- and mono-*ortho* CBs, in grey seals. Two second-dimension columns, LC-50 and VF-23 ms, had to

be used to avoid biased results. The enantiomeric fractions (EF), which may reflect differences in metabolic processes such as biotransformation or selective bioaccumulation, were determined for the CB 91, 95, 132, 149, and 174 pairs, and verified by GC×GC–ToF MS. Several pairs had EFs which deviated strongly from the racemic mixture value. Deviations were larger in grey seal liver than in blubber, which indicates enantioselective metabolism.

In a study of all 19 atropisomeric CB pairs, Chirasil-Dex combined with SupelcoWax-10 or VF-23ms gave the best results: seven out of the nine pairs of interest eluted without interference [29]. In a sheep cheese sample, eight out of nine—predominant—atropisomers were eluted free from interferences. In a subsequent paper [30], the EFs of eight atropisomeric CB pairs could be determined on Chirasil-Dex × Supelco-Wax-10. Enantio-enrichment was observed in several samples (milk, cheese, salmon).

Non-aromatic organohalogens Toxaphene, an insecticide widely used in the cotton-growing industry until its 1982 ban, is found in freshwater and marine biota all over the world. It is a very complicated mixture of, mainly, polychlorinated bornanes; many chlorocamphenes, chlorodihydrocamphenes, and chlorobornenes are present as minor compounds. Theoretically, several tens of thousands of congeners can be formed. Although most of these compounds will not be present in technical toxaphene (67–69 % chlorine), the quoted numbers nicely reflect the complexity that can be expected [118]. For the nomenclature of the toxaphene constituents, most authors use the 'Parlar system' which, unfortunately, provides no structural information and should, in future, be replaced by the 'Wester code' with its high information content [119, 120] (see [121]).

Prior to the introduction of GC×GC, the highest number of toxaphene constituents reported in the literature was 675 [122]. Calculating this number required time-consuming MDGC of the technical mixture; this involved pre-fractionation into 160 fractions followed by an about 30-min GC analysis of each of these. In marked contrast with this 3-day experiment, the first detailed GC×GC–μECD analysis of technical toxaphene on an HP-1 × HT-8 column set yielded a highly structured chromatogram which revealed the presence of over 1,000 constituents after a mere 2-h run [118]. Combination of this finding with the analysis of a mixture of 23 individual standard congeners and ToF MS evaluation convincingly demonstrated that the structuring occurs according to the number of chlorine substituents in a molecule, with the nature of the compounds—bornanes or camphenes—having little, if any, influence. Hepta- and octachlorinated congeners were found to represent some 75 % of the total toxaphene area.

Bordajandi et al. [123] used GC×GC–μECD to determine five environmentally relevant chiral toxaphene constituents, Parlars 26, 32, 40, 44, and 50, in commercial fish oil. A BGB-172 × BPX-50 column combination provided a complete separation of all five enantiomers. The LODs were low enough (2–6 ng/ml) to enable quantification of the enantiomers of the target compounds. EF calculations using heart-cut MDGC confirmed the racemic composition obtained by GC×GC for Parlars 26, 44, and 50. The analyte concentrations in the fish oils were in the

same range as those reported for fish, marine mammals, and human samples, with Parlars 50 and 26 as the most abundant congeners.

Polychlorinated *n*-alkanes (PCA) are complex mixtures with 30–70 % chlorine, and carbon chain lengths of $C_{10–13}$ (short-chain), $C_{14–17}$ (medium-chain), and $C_{17(+)}$ (long-chain). They are used as additives in a wide variety of industrial products and are present in many abiotic and biotic matrices. The main problem of PCA analysis is that in 1D-GC there is too little resolution: chromatograms display a characteristic broad envelope which indicates the presence of a large number of co-eluting peaks. The power of GC×GC to unravel the composition of PCA mixtures was first observed in a study on the use of ECNI qMS detection [44]. For a mixture of polychlorinated decanes with 65 % Cl, a well-ordered chromatogram was obtained. The bands could be assigned to hexa- to nonachlorodecanes. Such structure assignment would not have been possible when using EI-MS, because the spectra are then highly fragmented and provide little structural information.

In a more extensive characterization of PCAs on a DB-1 × 007-65 HT column set, and with ECNI ToF MS detection, several technical mixtures as well as 35 individual PCA standards were studied [54]. With a series of C_8Cl_2 to $C_{14}Cl_8$ standards it was observed that—due to closely similar polarity—compounds having the same chlorine substitution pattern but different carbon chain lengths were ordered as more or less parallel horizontal lines in the GC×GC plane. For some standards, e.g. 1,1,1,3,6,8,8,8-C_8Cl_8 and 1,2,5,6,9,10-$C_{10}Cl_6$, two or three closely contiguous peaks were observed due to the existence of diastereoisomers. As an example of the combined influence of number and position of the chlorine substituents, Fig. 13.9 shows GC×GC chromatograms for a technical short-chain PCA mixture and for mixtures of the main constituent classes, polychlorodecanes to polychlorotridecanes. The coloured lines connecting the peak apices are seen not to be straight in all cases due to further substructuring as a consequence of different substitution patterns within the homologue group. A mixture of short- and medium-chain PCAs was found in two household dust samples.

Other halogenated contaminants More recently, several studies were published on—next to PCBs and PCDD/Fs—polybrominated diphenyl ethers (PBDEs) and biphenyls (PBBs) as well as polychlorinated diphenyl ethers (PCDEs), terphenyls (PCTs), and naphthalenes (PCNs) and persistent organochlorine pesticides (OCPs). In one such study, which used GC×GC–ToF MS [124, 125], 59 target compounds in serum were separated in 50 min with a minimum number of co-elutions on DB-1 × HT-8. The second-dimension column helped to create an efficient separation from the matrix-related interfering background. A single analysis of a sample extract sufficed to identify and quantify all test compounds (method LODs, 1–15 ng/ml). OCP, PCB, and PBDE concentrations determined by the comprehensive technique and 1D-GC–HRMS showed good agreement with mutual differences of less than 20 % at concentrations above 1 ng/g of milk lipids.

In a paper on the within- and between-group separations of 12 classes of organohalogens, which included 126 PBDEs and essentially all compound classes mentioned above, a DB-1 first-dimension column was combined with 007-210,

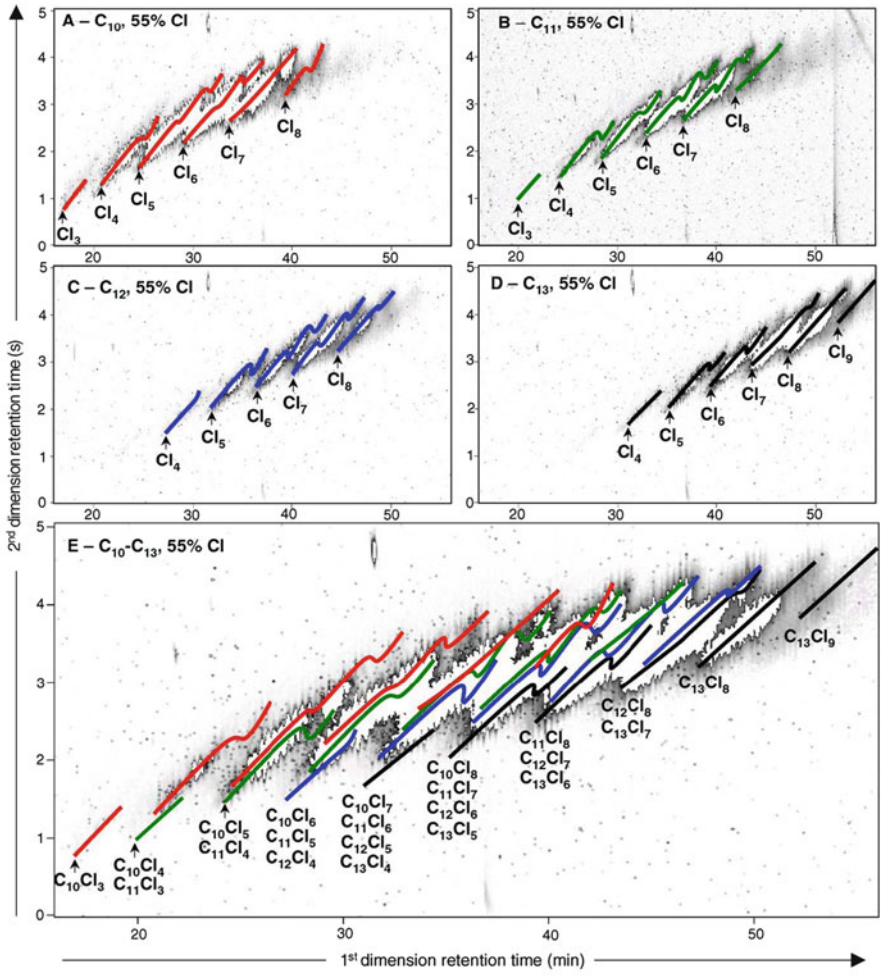

Fig. 13.9 GC×GC–ECNI–ToF MS chromatograms of polychlorinated (**a**) decanes, (**b**) undecanes, (**c**) dodecanes, (**d**) tridecanes, and (**e**) C_{10}–C_{13} technical mixture, all with 55 wt.% Cl, on DB-1×007-65HT column set. *Lines* indicate positions of apices within the bands [54]

HT-8, LC-50, 007-65HT, or VF-23ms in the second dimension [33]. Different sets of columns were found to give optimum results with regard to, e.g., between-group and within-group separations, separation of chlorinated and brominated analogues and of planar from non-planar groups of analytes. For example, with HT-8, GC×GC separation is mainly based on the number of halogen substituents, with 007-65HT PCAs and PBDEs effectively separated from all other compound classes tested (Fig. 13.10).

In another study [34] of the set of PBDEs quoted above, possible biodegradation products such as methoxy- and hydroxy-BDEs, and several fluorinated BDEs, were

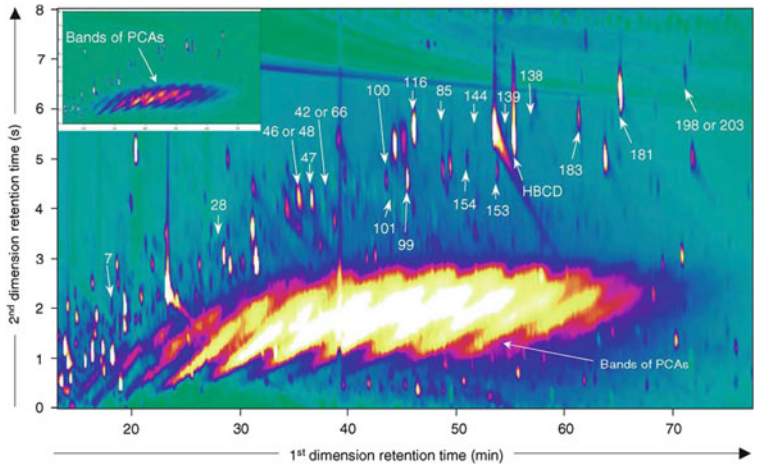

Fig. 13.10 GC×GC–μECD chromatogram of dust extract on DB-1×007-65HT column set for PCA and PBDE (indicated by number) determination. *Insert*: visualization with zoom-out z-scale [33]

included. All these compounds, and also a series of brominated flame retardants, eluted within the PBDE band. Apparently, the polarity differences between the parent PBDEs and the other analytes played no role in either the first- or second-dimension separation. However, the second-dimension selectivity caused all fluorinated BDEs to be efficiently separated from their parent compounds, making them likely internal standard candidates.

13.3.4 Environmental Studies

Selected recent papers on various types of environmental study are summarized in Table 13.4 [72, 187–201]. Several key studies are briefly discussed below.

Soils and sediments In order to assess the toxicity and, thus, the need for remediation, of oil-contaminated soils, a GC×GC–rapid-scanning qMS procedure was found to be a time-saving alternative to the routine Total Petroleum Hydrocarbon (TPM) GC–FID protocol [67]. Sample preparation is limited, fractionation problems are avoided, and detailed and specific chemical information is obtained. Detailed study of the experimental results showed that the GC×GC chromatogram can be read as a volatility—log K_{ow} matrix. Other work on contaminated soils [126, 127] convincingly showed that processes such as intrinsic biodegradation and engineered bioremediation can be adequately studied by means of GC×GC–FID, in one instance [127] combined with molecular-level ^{14}C analysis (to assess, in situ, microbial metabolism and cycling of carbon in the environment).

Table 13.4 Selected papers on GC×GC of micro-contaminants in environmental samples

Area of application	Detection	Ref.
Volatile compounds from marine salt	ToF MS	[187]
Identification of C10 derivatives of decalin	qMS	[72, 188]
Special surfactants in industrial cleaners	ToF MS	[189]
Environmental contaminants in household dust	ToF MS	[190]
Benzothiazoles, benzotriazoles, and benzosulfonamides in aqueous matrices	ToF MS	[191]
In situ measurements of organic aerosols	FID, qMS	[192]
Quantification of PAHs in urban dust and atmospheric particulates	ToF MS	[193]
Pesticides in animal feed, tobacco, tea, grapes; red grapefruit	ToF MS, qMS	[194–198]
Chemical profiling of illicit drug samples	FID, ToF MS	[199]
Chemical warfare agents in environmental samples	ToF MS	[200]
Powdered incense headspace and incense smoke	μECD/NPD, ToF MS	[201]

Air and aerosols Volatile organic compounds (VOCs) play a key role in the processes that generate urban photochemical smog and tropospheric ozone. GC×GC has turned out to be an excellent tool to determine the dominant reactive species involved. Already in an early study [128], a mere 40-min run on DB-1 × BPX-50 sufficed to observe over 550 VOCs. In a study on mono-aromatic complexity in urban air [129], close to 150 compounds were found—and 130 in gasoline. The chromatograms of air and gasoline vapour displayed almost identical distributions of C_3 and C_4 alkyl-substituted aromatic compounds. When partially oxidized organic compounds associated with PM2.5 aerosols were studied [130], DTD yielded an extremely complex chromatogram, with over 10,000 organic compounds being resolved in a single run. Because of the complexity, ordered structures were not immediately visible and the added selectivity of ToF MS detection was urgently required. An inventory of oxygenated VOCs (oVOCs) in a London aerosol based on this approach yielded 52 linear, 21 substituted and 64 cyclic oVOCs, and at least 100 oVOCs with longer chain lengths and increasing substitutions.

Online TD–GC×GC on BPX-5 × BPX-50 was combined with three detectors, i.e. high-resolution HR-ToF MS, and simultaneous NPD/qMS detection, to characterize atmospheric 29–58 nm particles. Exact mass measurement served to increase selectivity and group-type separation of, e.g., oxy-PAHs. For one group-type separation using 2D mass chromatograms, the sum of five selected ions was used: *m*/*z* 180.0575: 9H-fluoren-9-one, 1H-phenalene-1-one; *m*/*z* 194.0732: 9(10H)-anthracenone; *m*/*z* 198.0317: naphtho(1,2-c)furan-1,3-dione; *m*/*z* 230.0732: 7H-benz(de)anthracen-7-one, 11H-benzo(*a*)fluorene-11-one; and *m*/*z* 258.0681: naphthacene-5,12-dione, benz[*a*]anthrace-7,12-dione). NPD/qMS detection showed the presence of 15 *N*-containing compounds. Seven of these met the MS acceptance criteria and were identified by HR-ToF MS. TD–GC×GC–qMS, with a limited scan range of *m*/*z* 177–280 to achieve a data acquisition speed of 27 Hz, provided proper conditions for quantification [76].

In a project on in situ measurements of atmospheric VOCs, TD–GC×GC–FID showed the presence of several hundred well-separated peaks in air samples taken at a ground station on Crete [131, 132]. In order to facilitate peak identification, cartridge samples were collected and subjected to GC×GC–ToF MS. Some 650 peaks with S/N > 100 and *Sim* values of over 800 were identified. These included cyclic and acyclic alkanes, PAHs, oxygenated aromatics, alcohols, aldehydes, and ketones.

In order to facilitate interpretation of the more than 15,000 compounds detected in a PM2.5 sample, Welthagen et al. [76, 133] developed search criteria and rules to group peaks in the GC×GC chromatograms into distinct chemical classes, using ToF MS fragmentation patterns and GC×GC retention times. The example of Fig. 13.11 features some 10,000 peaks and indicates the seven groups that were identified, by colour coding. The bubble plot can be used for a rapid visual recognition of pattern changes in monitoring studies, as was convincingly demonstrated in a 3-year monitoring programme [133]. The same group published an automated compound classification for ambient aerosol sample separation using DTD–GC×GC–ToF MS [134]. Classifiers are based on fragmentation patterns and retention time, and mass spectral transformations are incorporated into software scripts.

Cigarette smoke Dallüge et al. [59] subjected mainstream cigarette smoke to GC×GC–ToF MS. Their paper discusses strategies that can be used when the focus of an analysis is on either target analytes, 'unknowns', or group-type separation [57]. A relevant flow chart is given in Fig. 13.12 (already referred to in Sect. 13.2.2). Automated data processing yielded 30,000 peaks having S/N > 30 in at least one extracted-ion trace. Peak finding and subsequent deconvolution plus library search could be performed fully automatedly. From amongst the 30,000 peaks (corresponding with some 7,500–10,000 compound names because of repeated modulation of, specifically, large fronting and/or tailing peaks), 20,000 peaks having too low match factors (*Sim* < 700; *Rev* < 850) were discarded. More than 1,500 peaks, or 520 compounds, had excellent (*Sim* > 800; *Rev* > 900) match factors and could easily be identified. For the other *ca*. 9,000 peaks with lower but still acceptable match factors, additional information was used to arrive at reliable identification. This included the use of linear RIs for the first-dimension separation—which added 660 peaks or 152 compounds to the list—and group-type information derived from the second-dimension retention times.

Chinese scientists used two column sets—non-polar × medium-polar and polar × non-polar—to study the acidic fraction of cigarette smoke condensate [52]. The former column combination gave properly structured chromatograms, while the latter set-up provided better peak shape for the organic acids. Using an approach similar to that discussed above, over 1,000 compounds with S/N > 100 were found. Automated data processing combined with manual identification led to the tentative identification of some 140 organic acids and over 150 phenols. In another paper, the number of tentatively identified phenols was even as high as 250, with alkylphenol, alkenylphenol, and naphthalenol derivatives each

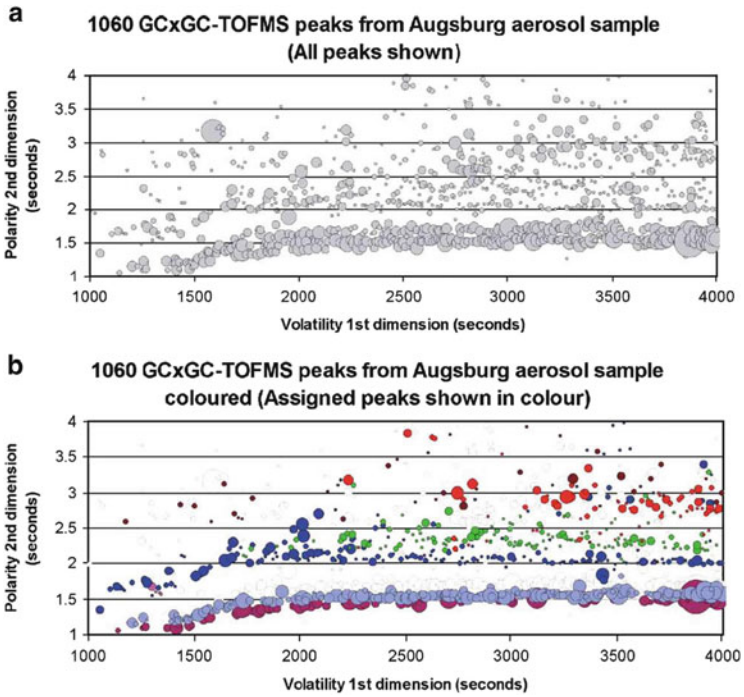

Fig. 13.11 GC×GC–ToF MS of aerosol sample. (**a**) Bubble plot of all peak apices used for grouping; with (**b**) indicating the identified groups. *Dark red*: alkanes; *light blue*: alkenes and cycloalkanes; *blue*: alkyl-substituted benzenes; *brown*: polar benzenes with or without alkyl substitution; *green*: hydrated naphthalenes and alkenyl benzenes; *red*: alkylated naphthalenes; *purple*: *n*-alkane acids [133]

contributing 50–60 entries [135]. With the basic fraction of the smoke condensate [136], ordered structures were obtained on the non-polar × medium-polar column set used, and 600 peaks were detected. Data processing revealed the presence of over 370 *N*-containing compounds, primarily pyridines and (iso)quinolines. For the characterization of complex hydrocarbons, the authors used GC combined with EI- and CI(+)-MS and GC×GC–ToF MS [137]. In the very complex non-polar neutral fraction some 4,000 peaks were detected and over 1,800 hydrocarbons were identified. The detection of over 100 isoprenoid hydrocarbons was of marked interest because isoprene is the basic unit of the terpenes, which may arise in tobacco via various pyrolysis and degradation pathways.

13.3.5 Petrochemical Analysis

Petrochemical samples are usually very complex and, unlike the situation encountered with other sample types, in most instances it is the matrix itself that has to be

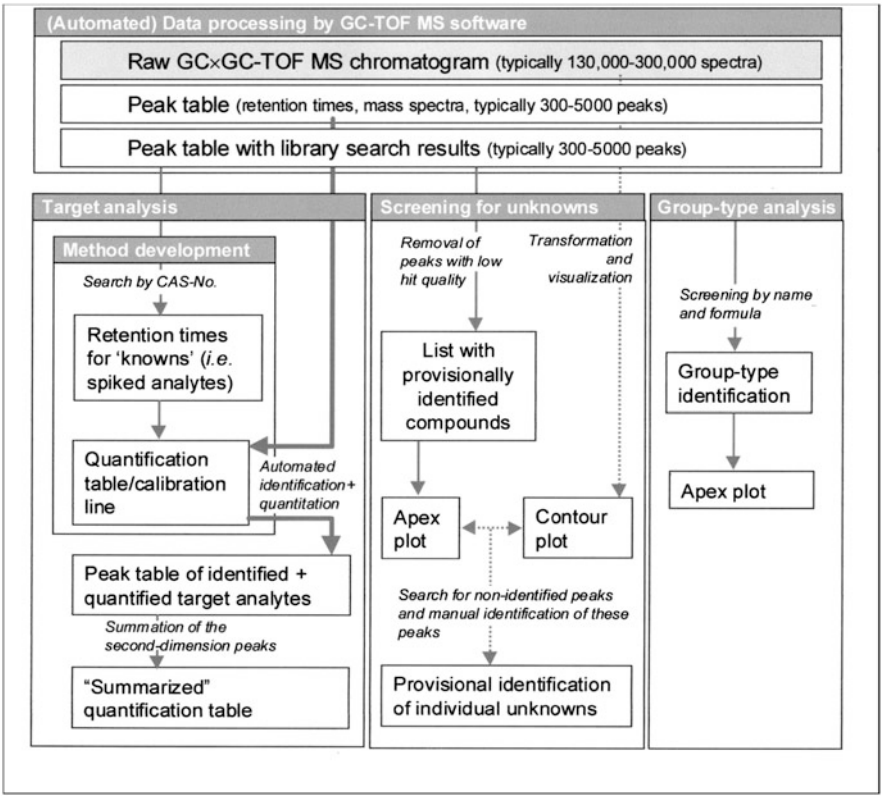

Fig. 13.12 Flow chart of ToF MS data-processing procedure. *Lines*: heavy—fully automated; *solid*—mainly automated; *dotted*—manual [57]

analysed. The constituents of petroleum (fractions) can be classified as hydrocarbons (C and H only) and hetero (containing S, N, O, V, Ni, and/or Fe) compounds. The former group can be subdivided into: (1) normal and branched (*iso*) acyclic alkanes or paraffins; (2) cyclic alkanes or naphthenes, with one or more saturated or naphthenic 5- or 6-membered rings—they may have one or more (branched) paraffins attached to the ring; (3) normal, branched, or cyclic unsaturated alkanes or alkenes, also called olefins—in general, crude oils or straight-run products do not contain olefins, but their content is often high in processed products obtained by thermal or catalytic cracking; and (4) aromatics, which can be subdivided into mono-, di-, and tri(+)-aromatics—they may have one or more paraffins or naphthenes attached to the ring system. Selected recent papers are included in Table 13.5 [75, 202–216]. Relevant information is presented below.

The compounds in most petrochemical samples are of a bewildering variety and their number is usually very large. No single 1D-GC operation can come up with a full separation [138, 139], and dedicated—but, unfortunately, complex and time-consuming—MDGC systems, such as the PIONA analyser referred to above, have to

Table 13.5 Selected papers on GC×GC of petrochemical products

Area of application	Detection	Ref.
Detailed characterization of middle distillates	FID	[202]
Online analysis of complex hydrocarbon mixtures	FID/ToF MS	[203]
Analysis of Fischer–Tropsch oil products	FID, ToF MS	[204]
Detailed analysis of light cycle oil	FID	[205, 206]
Characterization of aromatic compounds in extra heavy gas oil	ToF MS	[207]
N-containing compounds in heavy petroleum fractions	NCD	[208]
Biomarker characterization in oils	ToF MS	[75, 209]
Hydrocarbons up to *n*-C60 for analysis of vacuum gas oils	FID	[210]
Ecotoxicity of petroleum hydrocarbon mixtures in soil	FID	[211]
Basic and neutral nitrogen speciation in middle distillates	NCD	[212]
Petroleum hydrocarbon degradation in soil and leaching water	FID, ToF MS	[213]
Oxygenates in middle distillates: nature of biodiesel blends in diesel fuel	FID, ToF MS	[214]
Disentangling oil weathering	FID	[215, 216]

be used. Not surprisingly, therefore, characterization of petrochemical samples became the first application area of GC×GC. In one early study [140], analysis of a kerosene sample on a non-polar × polar column set yielded over 6,000 peaks. At that time, the first-dimension separation still took 8–9 h, with a modulation time of some 25 s. Less than a decade later, run times were down to 60–90 min with the, also today, standard modulation times of 6–8 s. As an illustration, Fig. 13.13 shows GC×GC–FID chromatograms of a light cycle oil and a non-aromatic solvent [141, 142]. With the oil, a key aspect is the very clear presence of ordered structures: six compound classes show up as distinct bands with, moreover, detailed substructures in each of these bands. That is, the potential of GC×GC for goals as diverse as fingerprinting, quantification of specific individual analytes, and group-type characterization is very clear. With the solvent, carefully reading the legend to the figure probably is the easiest way to appreciate the power of the comprehensive separation approach. The positions of two analytes, *n*-heptylcyclohexane and *n*-octylcyclopentane, are indicated to demonstrate that even features such as ring size and length or branching of alkyl substituents can be monitored.

GC×GC has been used also for the characterization of high-value petrochemical samples [143]. The separation of aromatics in products formed upon dehydrogenation of *n*-paraffins and of alcohols in Fischer–Tropsch products from the paraffinic matrix enabled their reliable quantification. The determination of 0.01 % of alkylbenzenes in the olefenic matrix of an oligomerization process is a good example of the potential of GC×GC. The authors also characterized middle distillates by using a polar × non-polar approach [144].

Other workers [145] combined NPLC on amino-based silica, with *n*-heptane as eluent, off-line with GC×GC on a DB-1 × BPX-50 column set. The aromaticity–volatility–polarity/ring structure separation provided information on the elution order of naphthenic and aromatic compounds which remain partly convoluted in GC×GC. Linear, mono-, di-, and even tri-naphthenic alkanes, which would have

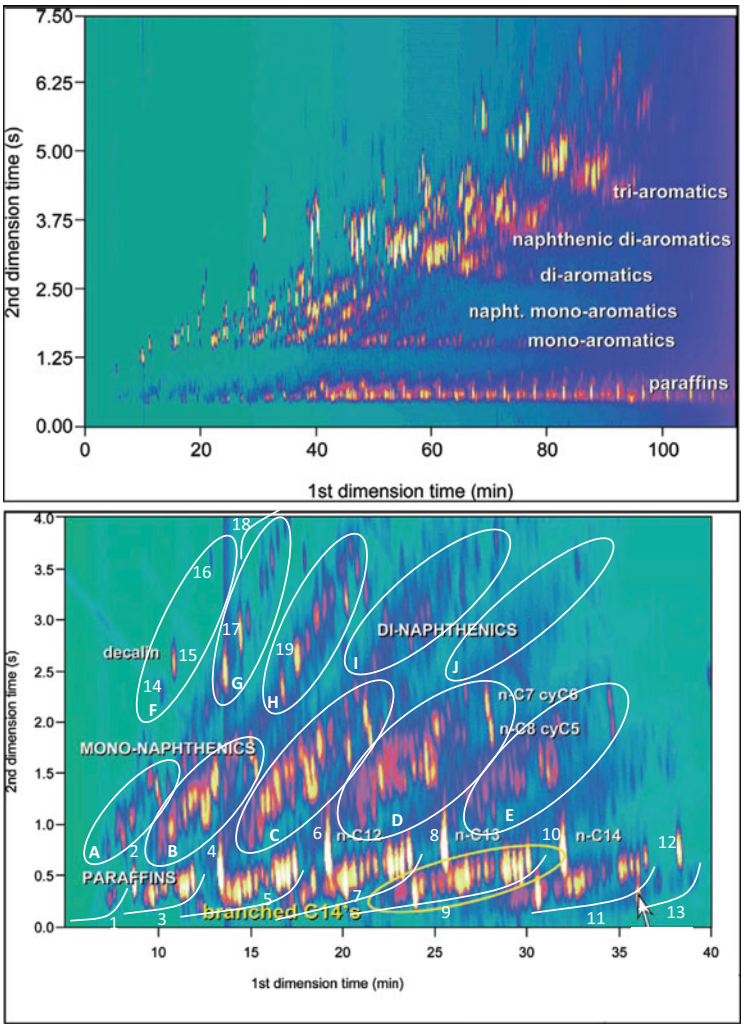

Fig. 13.13 GC×GC–FID of a light cycle oil on DB-1 × OV-1701 (*top*) and of a non-aromatic hydrocarbon solvent on CP Sil-2 CB × BPX-50 (*bottom*). (1–13) Alkanes, (1) branched C_{10}s, (2) *n*-C_{10}, (3) branched C_{11}s, (4) *n*-C_{11}, (5) branched C_{12}s; (6) *n*-C_{12}, (7) branched C_{13}s, (8) *n*-C_{13}, (9) branched C_{14}s, (10) *n*-C_{14}, (11) branched C_{15}s, (12) *n*-C_{15}, (13) branched C_{16}s, (14) unknown, (15) *trans*-decalin, (16) *cis*-decalin, (17) *trans*-methyldecalins, (18) *cis*-methyldecalins. A–E, mono-naphthenes C_{10}–C_{14}; F–J, di-naphthenes C_{10}–C_{13} [141, 142]

overlapped with mono-aromatic compounds in GC×GC, were resolved from each other and separated according to the number of rings. Admittedly, the dinaphthenes were less ordered than the linear and mononaphthenic alkanes, presumably because of the increasing number of isomers present (5- and 6-membered naphthenic rings and *cis*/*trans* isomerism).

GC×GC–FID was also used for the quantification of internal olefin or linear α-olefin contamination in petroleum samples [146]. With separate fine-tuned temperature programmes for the two columns, a 7.5 m Rtx-1 × 2 m BPX-50 column set yielded a fully acceptable separation of the alkene-based components in crude oils; C_{15}–C_{18} and C_{20} alkenes were determined.

The superiority of GC×GC–ToF MS over traditional GC–MS was demonstrated for the analysis of both the feed and the product from the hydrocracker coal liquefaction process. *n*-Alkanes and other saturates, which accumulate in the recycle solvent, could be identified in more detail, and the most desirable product fraction, corresponding to a naphtha or diesel fuel substitute, could be analysed. In addition, the numerous structural isomers of tetralin and methylindane, one important hydrogen donor/isomeric non-donor pair, were resolved [147].

In the field of hetero-atom-containing compounds, *S*- and *N*-containing compounds attract most attention. The former group, which comprises mercaptans, sulphides, and benzothiophenes, can cause bad odour, catalyst poisoning, and, in the case of fuels, environmental problems caused by conversion into SO_2 and SO_3. Basic nitrogen compounds, which are usually present in lower concentrations than the *S*-containing compounds, are notorious catalyst poisons.

Benzothiophenes (BTs) and related sulphur compounds often co-elute with the main groups of hydrocarbons in petrochemical samples, and selective detection is therefore required. Some early studies used ToF MS detection to analyse various oils and oil products [81, 148, 149] by recording properly selected extracted-ion chromatograms—e.g. the unique ions 161 and 178, or the molecular ions. A number of classes of alkyl-substituted BTs, dibenzothiophenes (DBTs), and benzonaphthothiophenes (BNTs) were identified and their substructures visualized. An alternative is to use SCD detection. Figure 13.14 shows a GC×GC–SCD chromatogram of a mixture of a light catalytically cracked cycle oil (LCCCO) and a heavy gas oil (HGO), demonstrating both the chemical class separation, inclusive of the roof-tiling, and the detection selectivity [150]. The high speed of the SCD allowed reliable quantification at a level of 25 mg/kg of total sulphur. In another study [46], the distribution of *S*-containing compounds in diesel oil from different types of crude oil (170–400 °C) was found to vary widely. Quantification in the mg/kg range (LODs, typically 0.01–0.02 mg/kg) was successful. In a crude oil over 3,600 peaks were detected: over 1,700 thiols/thioethers/disulphides/1-ring thiophenes, 950 BTs, and 700 DBTs.

GC×GC–SCD has been compared with standard methods employed in the petroleum industry, such as X-ray fluorescence (XRF), conventional GC–SCD, and HRMS, for the speciation of *S*-containing compounds in middle distillates [151]. The results were found to be similar to the standard XRF method for total sulphur content. In their turn, these two techniques are also similar to HRMS results for BT/DBT ratio determination. However, the comprehensive technique has the benefit of an excellent separation of the classes. This makes GC×GC the preferred tool for the quantification of individual components.

Wang et al. [47] used NCD detection to analyse a diesel sample after denitrogenation to approx. 20 μg/g nitrogen. The indoles and carbazoles showed

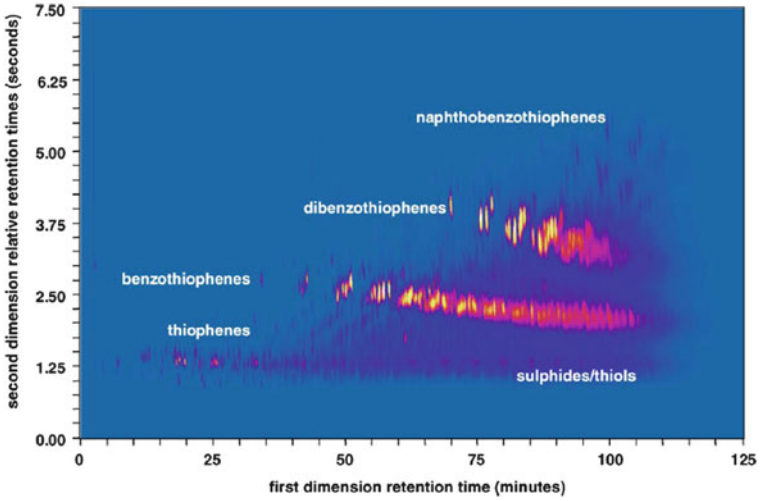

Fig. 13.14 GC×GC–SCD chromatogram of an LCCCO–HGO mixture on DB-1 × BPX-50 column set [150]

up as distinct bands, with a further roof-tile subdivision within these bands: C_0–C_6 alkyl-substituted indoles and C_0–C_5 alkyl-substituted carbazoles could be clearly distinguished, and quantification of these subgroups was satisfactory. In a GC×GC–NCD analysis of all *N*-containing compounds in middle distillates on, preferably, SPB-5 × Solgel Wax, all classes of compounds were found to be organized into distinct bands, with a further isomer-based subdivision [48]. As regards quantification, the comprehensive approach showed higher precision than 1D-GC and prevented incorrect results caused by a lack of resolution. For instance, indole and quinoline derivatives cannot be discriminated when conventional GC is used. The GC×GC–NCD data for basic and neutral nitrogen contents were in excellent agreement with those obtained by the ASTM.

13.4 Conclusions

All recent reviews state that GC×GC is, today, a mature technique [43, 152]. This is also borne out by the large number of papers devoted to it in [153] which is dedicated to the Riva del Garda (Italy) GC×GC symposium of 30 May/4 June 2010. In the past few years, GC×GC publications have shifted in focus, with more emphasis on the development of applications, and much less on that of instrumentation. The technique is increasingly being applied in research laboratories, in academia, governmental institutes, and industry. The types of application vary widely, and include group-type identification and quantification, general fingerprinting, the unravelling of the composition of highly complex mixtures, and recognition plus identification of individual known as well as unknown (marker) analytes.

One aspect of interest is that the application of GC×GC instead of 1D-GC techniques has not led to a significant simplification of sample preparation procedures, as was initially predicted by many workers in the field but has, rather, served to demonstrate the very high—and, often, unexpected—complexity of many sample types. The analysis of air and aerosols and of cigarette smoke and petrochemical products and the successful studies of the composition of technical organochlorine products and of flavours and fragrances are a few obvious examples.

Another aspect of interest is that, from among the many detectors used in GC×GC, three have emerged as essential tools. The FID has lost its early dominant position but still is a much appreciated general workhorse and is widely applied in the (group-type) analyses of petrochemical products. The very sensitive micro-ECD is virtually indispensable for all work concerning organohalogens where selective (ultra-)trace screening frequently is essential. It is, however, MS-based detection that at present is of most importance and, to our opinion, will continue to be so for the next 5–10 years. ToF MS detection is extremely powerful, versatile and wide ranging, and, consequently, the preferred approach. For many less demanding applications—and, especially, for those that do not involve a search for unknowns—rapid-scanning qMS is an interesting alternative.

In summary, GC×GC is a powerful and widely applicable analytical technique, which derives much of its potential from (1) its high 2D chromatographic separation power, (2) the creation of ordered structures which facilitate analyte classification and even preliminary identification, and (3) reliable and rapid, almost invariably ToF MS-based, identification. There are two main challenges still ahead of us, i.e. further exploration of the chemical information revealed by the 2D-GC separations, and improving the now often too time-consuming data handling plus interpretation of the huge number of peaks typically showing up in a GC×GC chromatogram.

References

1. Giddings JC (1990) In: Cortes HJ (ed) Multidimensional chromatography, techniques and applications. Marcel Dekker, New York, pp 1–27
2. Simmons MC, Snyder L (1958) Anal Chem 30:32–35
3. Marriott PJ (2000) In: Wilson ID (ed) Encyclopedia of separation science, vol 2. Academic, San Diego, pp 536–544
4. Schomburg G (1995) J Chromatogr A 703:309–325
5. Bertsch W (2000) In: Meyers RA (ed) Encyclopedia of analytical chemistry, vol 12. Wiley, Chichester, UK, pp 10698–10723
6. Boer H, van Arkel P (1971) Chromatographia 4:300–308
7. van Arkel P, Beens J, Spaans H, Grutterink D, Verbeek R (1988) J Chromatogr Sci 25:141–148
8. Hess P, de Boer J, Cofino WP, Leonards PEG, Wells DE (1995) J Chromatogr A 703:417–465
9. Campo E, Ferreira V, López R, Escudero A, Cacho J (2006) J Chromatogr A 1122:202–208

10. Oostdijk JP, Degenhardt CEAM, Trap HC, Langenberg JP (2007) J Chromatogr A 1150:62–69
11. Schmarr H-G, Ganss S, Sang W, Potouridis T (2007) J Chromatogr A 1150:78–84
12. Liu Z, Phillips JB (1991) J Chromatogr Sci 29:227–231
13. Giddings JC (1987) J High Resolut Chromatogr 10:319–323
14. Marriott PJ, Kinghorn RM (1999) Trends Anal Chem 18:114–125
15. Kristenson EM, Korytár P, Danielsson C, Kallio M, Brandt M, Mäkelä J, Vreuls JJR, Beens J, Brinkman UAT (2003) J Chromatogr A 1019:65–77
16. Bueno PA Jr, Seeley JV (2004) J Chromatogr A 1027:3–10
17. Tranchida PQ, Purcaro G, Dugo P, Mondello L (2011) Trends Anal Chem 30:1437–1461
18. Ryan D, Morrison P, Marriott PJ (2005) J Chromatogr A 1071:47–53
19. Dimandja JMD, Clouden GC, Colón I, Focant JF, Cabey WV, Parry RC (2003) J Chromatogr A 1019:261–272
20. de Geus HJ, Aidos I, de Boer J, Luten JB, Brinkman UAT (2001) J Chromatogr A 910:95–103
21. Korytár P, Leonards PEG, de Boer J, Brinkman UAT (2002) J Chromatogr A 958:203–218
22. Mondello L, Casilli A, Tranchida PQ, Dugo P, Costa R, Festa S, Dugo G (2004) J Sep Sci 27:442–450
23. Adahchour M, Beens J, Vreuls RJJ, Batenburg AM, Brinkman UAT (2004) J Chromatogr A 1054:47–55
24. Mayadunne R, Nguyen T-T, Marriott PJ (2005) Anal Bioanal Chem 382:836–847
25. Harynuk J, Górecki T (2006) J Chromatogr A 1105:159–167
26. Wu J, Lu X, Tang W, Kong H, Zhou S, Xu G (2004) J Chromatogr A 1034:199–205
27. Shao Y, Marriott PJ (2003) Anal Bioanal Chem 375:635–642
28. Williams A, Ryan D, Guasca AO, Marriott PJ, Pang E (2005) J Chromatogr B 817:97–107
29. Bordajandi LR, Korytár P, de Boer J, Gonzalez MJ (2005) J Sep Sci 28:163–171
30. Bordajandi LR, Ramos L, González MJ (2003) J Chromatogr A 1078:128–135
31. Harju M, Bergman A, Olsson M, Roos A, Haglund P (2003) J Chromatogr A 1019:127–142
32. Koblizková M, Dusek L, Jarkovsky J, Hofman J, Bucheli TD, Klanova J (2008) Environ Sci Technol 42:5978–5984
33. Korytár P, Leonards PEG, de Boer J, Brinkman UAT (2005) J Chromatogr A 1086:29–44
34. Korytár P, Covaci A, Leonards PEG, de Boer J, Brinkman UAT (2005) J Chromatogr A 1100:200–207
35. Harynuk J, Wynne PM, Marriott PJ (2006) Chromatographia 63:S61–S66
36. Seeley JV, Kramp FJ, Sharpe KS, Seeley SK (2002) J Sep Sci 25:53–59
37. Adahchour M, Jover E, Beens J, Vreuls RJJ, Brinkman UAT (2005) J Chromatogr A 1086:128–134
38. Sinha AE, Hope JL, Prazen BJ, Fraga CG, Nilsson EJ, Synovec RE (2004) J Chromatogr A 1056:145–154
39. Frysinger GS, Gaines RB (1999) J High Resolut Chromatogr 22:251–255
40. Beens J, Janssen H-G, Adahchour M, Brinkman UAT (2005) J Chromatogr A 1086:141–150
41. Harynuk J, Górecki T (2005) J Chromatogr A 1086:135–140
42. Zhu Z, Harynuk J, Górecki T (2005) J Chromatogr A 1105:17–24
43. Adahchour M, Beens J, Brinkman UAT (2008) J Chromatogr A 1186:67–108
44. Korytár P, Parera J, Leonards PEG, de Boer J, Brinkman UAT (2005) J Chromatogr A 1067:255–264
45. Hua R, Li Y, Liu W, Zheng J, Wei H, Wang J, Lu X, Kong H, Xu G (2003) J Chromatogr A 1019:101–109
46. Hua R, Wang J, Kong H, Liu J, Lu X, Xu G (2004) J Sep Sci 27:691–698
47. Wang FCY, Robbins WK, Greaney MA (2004) J Sep Sci 27:468–472
48. Adam F, Bertoncini F, Brodusch N, Durand E, Thiébaut D, Espinat D, Hennion MC (2007) J Chromatogr A 1148:55–64
49. Khummueng W, Trenerry C, Rose G, Marriott PJ (2006) J Chromatogr A 1131:203–214

50. van Stee LLP, Beens J, Vreuls RJJ, Brinkman UAT (2003) J Chromatogr A 1019:89–99
51. Kallio M, Hyötyläinen M, Lehtonen TM, Jussila M, Hartonen K, Shimmo M, Riekkola ML (2003) J Chromatogr A 1019:251–260
52. Lu X, Cai J, Kong H, Wu M, Hua R, Zhao M, Liu J, Xu G (2003) Anal Chem 75:4441–4451
53. Hao C, Headley JV, Peru KM, Frank R, Yang P, Solomon KR (2005) J Chromatogr A 1067:277–284
54. Korytár P, Parera J, Leonards PEG, Santos FJ, de Boer J, Brinkman UAT (2005) J Chromatogr A 1086:71–82
55. Baier H-U, Bohme S (2009) Shimadzu, comprehensive GC×GC(q)MS with negative chemical ionisation: PCBs in Bovine Fat. see http://chromatographyonline.findanalytichem.com/lcgc/data/articlestandard//lcgc/382009/627270/article.pdf
56. Dück R, Wulf V, Geißler M, Baier H-U, Wirtz M, Kling H-W, Gäb S, Shmitz OJ (2010) Anal Bioanal Chem 396:2273–2283
57. Dallüge J, Vreuls RJJ, Beens J, Brinkman UAT (2002) J Sep Sci 25:201–214
58. Dallüge J, van Rijn M, Beens J, Vreuls RJJ, Brinkman UAT (2002) J Chromatogr A 965:207–217
59. Dallüge J, van Stee LLP, Xu X, Williams J, Beens J, Vreuls RJJ, Brinkman UAT (2002) J Chromatogr A 974:169–184
60. Mitschke S, Welthagen W, Zimmermann R (2006) Anal Chem 78:6364–6375
61. Welthagen W, Mitschke S, Mulberger F, Zimmermann R (2007) J Chromatogr A 1150:54–61
62. Debonneville C, Chaintreau A (2004) J Chromatogr A 1027:109–115
63. Ryan D, Shellie R, Tranchida P, Casilli A, Mondello L, Marriott PJ (2004) J Chromatogr A 1054:57–65
64. Adahchour M, Brandt M, Baier H-U, Vreuls RJJ, Batenburg AM, Brinkman UAT (2005) J Chromatogr A 1067:245–254
65. Mondello L, Casilli A, Tranchida PQ, Dugo G, Dugo P (2005) J Chromatogr A 1067:235–243
66. Cordero C, Bicchi C, Joulain D, Rubiolo P (2007) J Chromatogr A 1150:37–49
67. van de Weghe H, Vanermen G, Gemoets J, Lookman R, Bertels D (2006) J Chromatogr A 1137:91–100
68. Tranchida PQ, Purcaro G, Fanali C, Dugo P, Dugo G, Mondello L (2010) J Chromatogr A 1217:4160–4166
69. Schmarra H-G, Bernhardt J (2010) J Chromatogr A 1217:565–574
70. Schmarra H-G, Gan S, Koschinski S, Fischer U, Riehle C, Kinnart U, Potouridis T, Kutyrev M (2010) J Chromatogr A 1217:6769–6777
71. Schmarra H-G, Bernhardt J, Fischer U, Stephan A, Müller P, Durner D (2010) Anal Chim Acta 672:114–123
72. Piccolo L, Nassreddine S, Toussaint G, Geantet C (2010) J Chromatogr A 1217:5872–5873
73. Gu Q, David F, Lynen F, Rumpel K, Xu G, de Vos P, Sandra P (2010) J Chromatogr A 1217:4448–4453
74. Poliak M, Fialkov AB, Amirav A (2008) J Chromatogr A 1210:108–114
75. Aguiar A, Júnior AIS, Azevedo DA, Neto FRA (2010) Fuel 89:2760–2768
76. Ochiai N, Ieda T, Sasamoto K, Fushimi A, Hasegawa S, Tanabe K, Kobayashi S (2007) J Chromatogr A 1150:13–20
77. Shunji H, Yoshikatsu T, Akihiro F, Hiroyasu I, Kiyoshi T, Yasuyuki S, Masa-aki U, Akihiko K, Kazuo T, Hideyuki O, Katsunori A (2008) J Chromatogr A 1178:187–198
78. Patterson DG Jr, Welch SM, Turner WE, Sjödin A, Focant J-F (2011) J Chromatogr A 1218:3274–3281
79. Adahchour M, Beens J, Vreuls RJJ, Brinkman UAT (2006) Trends Anal Chem 25:540–553
80. Lee AL, Bartle KD, Lewis AC (2001) Anal Chem 73:1330–1335
81. Dallüge J, Beens J, Brinkman UAT (2003) J Chromatogr A 1000:69–108
82. Pierce KM, Hoggard JC, Mohler RE, Synovec RE (2008) J Chromatogr A 1184:341–352
83. Reichenbach SE (2009) In: Ramos L (ed) Comprehensive two dimensional gas chromatography. Elsevier, Amsterdam, Ch. 4

84. Hoggard JC, Synovec RE (2009) In: Ramos L (ed) Comprehensive two dimensional gas chromatography. Elsevier, Amsterdam, Ch. 5
85. Ramos L (2009) Comprehensive two dimensional gas chromatography. Elsevier, Amsterdam
86. Adahchour M, Beens J, Vreuls RJJ, Brinkman UAT (2006) Trends Anal Chem 25:438–454
87. Górecki T, Panic O, Oldridge N (2006) J Liq Chromatogr Relat Technol 29:1077–1104
88. Mondello L, Casilli A, Tranchida PQ, Dugo P, Dugo G (2003) J Chromatogr A 1019:187–196
89. Mondello L, Tranchida PQ, Dugo P, Dugo G (2006) J Pharm Biomed Anal 41:1566–1570
90. Jover E, Adahchour M, Bayona JM, Vreuls RJJ, Brinkman UAT (2005) J Chromatogr A 1086:2–11
91. de Koning S, Janssen HG, Brinkman UAT (2006) LC–GC Eur 19:590–597
92. Adahchour M, van Stee LLP, Beens J, Vreuls RJJ, Batenburg MA, Brinkman UAT (2003) J Chromatogr A 1019:157–172
93. Adahchour M, Wiewel J, Verdel R, Beens J, Vreuls RJJ, Batenburg AM, Brinkman UAT (2005) J Chromatogr A 1086:99–106
94. Shellie RA, Marriott PJ, Chaintreau A (2004) Flavour Fragr J 19:91–98
95. David F, Devos Ch, Sandra P (2006) LC–GC Eur 19:602–616
96. Zellner BD, Casilli A, Dugo P, Dugo G, Mondello L (2007) J Chromatogr A 1141:279–286
97. Özel MZ, Gogus F, Hamilton JF, Lewis AC (2004) Chromatographia 60:79–83
98. Gogus F, Özel MZ, Lewis AC (2006) J Sep Sci 29:1217–1222
99. Zhu Sh LX, Dong L, Xing J, Su X, Kong H, Xu G, Wu C (2005) J Chromatogr A 1086:107–114
100. Wu JF, Lu X, Tang WY, Lian XH, Kong HW, Ruan CH, Xu GW (2004) Chem J Chin Univ 25:1432–1437
101. Wu HF, Lu X, Tang WY, Kong HW, Zhou SF, Xu GW (2004) Chin J Anal Chem 32:582–586
102. Roberts MT, Dufour JP, Lewis AC (2004) J Sep Sci 27:473–478
103. Özel MZ, Gogus F, Lewis AC (2006) J Chromatogr A 1114:164–169
104. Cardeal ZL, Gomes da Silva MDR, Marriott PJ (2006) Rapid Commun Mass Spectrom 20:2823–2836
105. Rochat S, de Saint Laumer JY, Chaintreau A (2007) J Chromatogr A 1147:85–94
106. Sanchez JM, Sacks RD (2006) Anal Chem 78:3046–3054
107. Libardoni M, Stevens PT, Hunter Waite J, Sack R (2006) J Chromatogr B 842:13–21
108. Welthagen W, Shellie RA, Spranger J, Ristow M, Zimmermann R, Fiehn O (2005) Metabolomics 1:65–73
109. Shellie RA, Welthagen W, Zrostlikova J, Spranger J, Ristow M, Fiehn O, Zimmermann R (2005) J Chromatogr A 1086:83–90
110. Mohler RE, Dombek KM, Hoggard JC, Young ET, Synovec RE (2006) Anal Chem 78:2700–2709
111. Pierce KM, Hope JL, Hoggard JC, Synovec RE (2006) Talanta 70:797–804
112. Kalinova B, Jiros P, Zdarek J, Wen X, Hoskovec M (2006) Talanta 69:542–547
113. de Geus HJ, de Boer J, Brinkman UAT (2002) Chromatographia 55:339–344
114. Harju M, Danielsson C, Haglund P (2003) J Chromatogr A 1019:111–126
115. Hoh E, Mastovska K, Lehotay SJ (2007) J Chromatogr A 1145:210–221
116. Focant JF, Reiner EJ, MacPherson K, Kolic T, Sjödin A, Patterson DG Jr, Reese SL, Dorman FL, Cochran J (2004) Talanta 63:1231–1240
117. Danielsson C, Wiberg K, Korytár P, Bergek S, Brinkman UAT, Haglund P (2005) J Chromatogr A 1086:61–70
118. Korytár P, van Stee LLP, Leonards PEG, de Boer J, Brinkman UAT (2003) J Chromatogr A 994:179–189
119. Wester PG, Geus HJ, de Boer J, Brinkman UAT (1997) Chemosphere 35:1187–1194
120. Wester PG, de Geus HJ, de Boer J, Brinkman UAT (1997) Chemosphere 35:2857–2860
121. de Geus HJ (2002) PhD Thesis, Free University of Amsterdam, Amsterdam, the Netherlands
122. Dunn M, Shellie R, Morrison P, Marriott PJ (2004) J Chromatogr A 1056:163–169
123. Bordajandi LR, Ramos L, Gonzalez MJ (2006) J Chromatogr A 1125:220–228

124. Focant JF, Sjödin A, Patterson DG Jr (2003) J Chromatogr A 1019:143–156
125. Focant JF, Sjödin A, Turner WE, Patterson DG (2004) Anal Chem 76:6313–6320
126. Penet S, Vendeuvre C, Bertoncini F, Marchal R, Monot F (2006) Biodegradation 17:577–585
127. Slater GF, Nelson RK, Kile BM, Reddy CM (2006) Org Geochem 37:981–989
128. Lewis AC, Carslaw N, Marriott PJ, Kinghorn RM, Morrison P, Lee AL, Bartle KD, Pilling MJ (2000) Nature 405:778–781
129. Hamilton JF, Lewis AC (2003) Atmos Environ 37:589–602
130. Hamilton JF, Webb PJ, Lewis AC, Hopkins JR, Smith S, Davy P (2004) Atmos Chem Phys 4:1279–1290
131. Shimmo M, Hyötyläinen T, Kallio M, Antifa P, Riekkola ML (2004) LC–GC Eur 17:640–645
132. Xu X, van Stee LLP, Williams J, Beens J, Adahchour M, Vreuls RJJ, Brinkman UAT, Lelieveld J (2003) Atmos Chem Phys 3:665–682
133. Welthagen W, Schnelle-Kreis J, Zimmermann R (2003) J Chromatogr A 1019:233–249
134. Vogt L, Groger T, Zimmermann R (2007) J Chromatogr A 1150:2–12
135. Lu X, Cai JL, Wu JF, Kong HW, Zhao MY, Hua RX, Liu JF, Xu GW (2004) Acta Chim Sin 62:804–810
136. Lu X, Zhao M, Kong H, Cai J, Wu J, Wu M, Hua R, Liu J, Xu G (2004) J Sep Sci 27:101–109
137. Lu X, Zhao M, Kong H, Cai J, Wu J, Wu M, Hua R, Liu J, Xu G (2004) J Chromatogr A 1043:265–273
138. Marriott PJ, Morrison PD, Shellie RA, Dunn MS, Sari E, Ryan D (2003) LC−GC Eur (December) 2–10
139. Shellie RA, Marriott PJ, Morrison P, Mondello L (2004) J Sep Sci 27:504–512
140. Venkatramani CJ, Phillips JB (1993) J Microcol Sep 5:511–516
141. Beens J, Blomberg J, Schoenmakers PJ (2000) J High Resolut Chromatogr 23:182–188
142. Blomberg J (2002) PhD Thesis, Free University of Amsterdam, Amsterdam, the Netherlands
143. Vendeuvre C, Bertoncini F, Duval L, Duplan JL, Thiébaut D, Hennion MC (2004) J Chromatogr A 1056:155–162
144. Vendeuvre C, Ruiz-Guerrero R, Bertoncini F, Duval L, Thiébaut D, Hennion MC (2005) J Chromatogr A 1086:21–28
145. Edam R, Blomberg J, Janssen HG, Schoenmakers PJ (2005) J Chromatogr A 1086:12–20
146. Reddy CM, Nelson RK, Sylva SP, Xu L, Peacock EE, Raghuraman B, Mullins OC (2007) J Chromatogr A 1148:100–107
147. Hamilton JF, Lewis AC, Millan M, Bartle KD, Herod AA, Kandiyoti R (2007) Energ Fuels 21:286–294
148. Ryan D, Marriott PJ (2003) Anal Bioanal Chem 376:1939–1943
149. van Deursen M (2002) PhD Thesis, Technical University of Eindhoven, Eindhoven, the Netherlands
150. Blomberg J, Riemersma T, van Zuijlen M, Chaaban H (2004) J Chromatogr A 1050:77–84
151. Rosario RG, Colombe V, Didier T, Fabrice B, Didier E (2006) J Chromatogr Sci 44:566–573
152. Adahchour M, Beens J, Vreuls RJJ, Brinkman UAT (2006) Trends Anal Chem 25:821–840
153. Rikkola M.-L (2011) J Chromatogr A 1218(21):3129–3406
154. Villegas C, Zhao Y, Curtis JM (2010) J Chromatogr A 1217:775–784
155. Stanimirova I, Üstün B, Čajka T, Riddellová K, Hajslová J, Buydens LMC, Walczak B (2010) Food Chem 118:171–176
156. Čajka T, Hajslová J, Pudil F, Riddellová K (2009) J Chromatogr A 1216:1458–1462
157. Čajka T, Hajšlová J, Cochran J, Holadová K, Klimnková E (2007) J Sep Sci 30:534–546
158. Čajka T, Riddellová K, Klimanková E, Cerna M, Pudil F, Hajslová J (2010) Food Chem 121:282–289
159. Vaz-Freire LT, da Silva MDRG, Freitas AMC (2009) Anal Chim Acta 633:263–270
160. Özel MZ, Gogus F, Yagci S, Hamilton JF, Lewis AC (2010) Food Chem Toxicol 48:3268–3273

161. de Souza PP, Cardeal ZL, Augusti R, Morrison P, Marriott PJ (2009) J Chromatogr A 1216:2881–2890
162. Cardeal ZL, Marriott PJ (2009) Food Chem 112:747–755
163. Cardeal ZL, de Souza PP, da Silva MDRG, Marriott PJ (2008) Talanta 74:793–799
164. Ratel J, Engel E (2009) J Chromatogr A 1216:7889–7898
165. Lojzova L, Riddellová K, Hajslová J, Zrostlikova J, Schurek J, Čajka T (2009) Anal Chim Acta 641:101–109
166. Tranchida PQ, Purcaro G, Conte L, Dugo P, Dugo G, Mondello L (2009) J Chromatogr A 1216:7301–7306
167. Cordero C, Bicchi C, Rubiolo P (2008) J Agric Food Chem 56:7655–7666
168. Bianchi F, Careri M, Conti C, Musci M, Vreuls RJJ (2007) J Sep Sci 30:527–533
169. von Muhlen C, Zini CA, Caramao EB, Marriott PJ (2008) J Chromatogr A 1200:34–42
170. Eyres GT, Marriott PJ, Dufour J-P (2007) J Agric Food Chem 55:6252–6261
171. Kouremenos KA, Pitt J, Marriott PJ (2010) J Chromatogr A 1217:104–111
172. Mitrevski BS, Wilairat P, Marriott PJ (2010) J Chromatogr A 1217:127–135
173. van der Meer JA, Trap HC, Noort D, van der Schans MJ (2010) J Chromatogr B 878:1320–1325
174. Windt M, Meier D, Marsman JH, Heeres HJ, de Koning S (2009) J Anal Appl Pyrol 85:38–46
175. Li X, Xu Z, Lu X, Yang X, Yin P, Kong H, Yu Y, Xu G (2009) Anal Chim Acta 633:257–262
176. Amorim LCAA, Dimandja J-M, Cardeal ZL (2009) J Chromatogr A 1216:2900–2904
177. Kaal E, de Koning S, Brudin S, Janssen H-G (2008) J Chromatogr A 1201:169–175
178. LECO Corporation (2008) Saint Joseph, MI, USA, see http://www.leco.com/resources/application_notes/pdf/PEG_LIVER_DRUG-INDUCED_INJURY_URINE_203-821-302.pdf
179. Kusano M, Fukushima A, Kobayashi M, Hayashi N, Jonsson P, Moritz T, Ebana K, Saito K (2007) J Chromatogr B 855:71–79
180. Lacorte S, Ikonomou MG, Fischer M (2010) J Chromatogr A 1217:337–347
181. Hoh E, Lehotay SJ, Pangallo KC, Mastovska K, Ngo HL, Reddy CM, Vetter W (2009) J Agric Food Chem 57:2653–2660
182. Memersheimerová JM, Tienpont B, David F, Krupčik J, Sandra P (2009) J Chromatogr A 1216:6043–6062
183. Robrock KR, Korytár P, Cohen LA (2008) Environ Sci Technol 42:2845–2852
184. Pangallo K, Nelson RK, Teuten EL, Pedler BE, Reddy CM (2008) Chemosphere 71:1557–1565
185. Bordajandi LR, Ramos JJ, Sanz J, Gonzalez MJ, Ramos L (2008) J Chromatogr A 1186:312–324
186. Hoh E, Lehotay SJ, Mastovska K, Huwe JK (2008) J Chromatogr A 1201:69–77
187. Silva I, Rocha SM, Coimbra MA, Marriott PJ (2010) J Chromatogr A 1217:5511–5521
188. Flego C, Gigantiello N, Parker WO, Calemma V (2009) J Chromatogr A 1216:2891–2899
189. Wulf V, Wienand N, Wirtz M, Kling H-W, Gäb S, Schmitz OJ (2010) J Chromatogr A 1217:749–754
190. Hilton DC, Jones RS, Sjöind A (2010) J Chromatogr A 1217:6851–6856
191. Jover E, Matamoros V, Bayona JM (2009) J Chromatogr A 1216:4013–4019
192. Goldstein AH, Worton DR, Williams BJ, Hering SV, Kreisberg NM, Panic O, Górecki T (2008) J Chromatogr A 1186:340–347
193. Muňoz O, Pietrini RV, Pina AA, Tran TC, Morrison P, Marriott PJ (2008) J Chromatogr A 120:161–168
194. van der Lee MK, van der Weg G, Traag WA, Mol HGJ (2008) J Chromatogr A 1186:325–339
195. Cochran J (2008) J Chromatogr A 1186:202–210
196. Schurek J, Portolés T, Hajslová J, Riddellová K, Hernández F (2008) Anal Chim Acta 611:163–172
197. Banerjee K, Patil SH, Dasgupta S, Oulkar DP, Patil SB, Savant R, Adsule PG (2008) J Chromatogr A 1190:350–357

198. Mondello L, Casilli A, Tranchida PQ, Presti ML, Dugo P, Dugo G (2007) Anal Bioanal Chem 389:1755–1763
199. Gröger T, Schäffer M, Pütz M, Ahrens B, Drew K, Eschner M, Zimmermann R (2008) J Chromatogr A 1200:8–16
200. Trap HC, van der Schans M (2007) LC–GC Eur 20:202–207
201. Tran TC, Marriott PJ (2008) Atmos Environ 42:7360–7372
202. Adam F, Thiébaut D, Bertoncini F, Courtiade M, Hennion M-C (2010) J Chromatogr A 1217:1386–1394
203. van Geem KM, Pyla SP, Reyniers M-F, Vercammen J, Beens J, Marina GB (2010) J Chromatogr A 1217:6623–6633
204. van der Westhuizen R, Potgieter H, Prinsloo N, de Villiers A, Sandra P (2011) J Chromatogr A 1218:3173–3179
205. van der Westhuizen R, Crous R, de Villiers A, Sandra P (2010) J Chromatogr A 1217:8334–8339
206. Semard G, Gouin C, Bourdet J, Bord N, Livadaris V (2011) J Chromatogr A 1218:3146–3152
207. Ávila BMF, Pereira R, Gomes AO, Azevedo DA (2011) J Chromatogr A 1216:3208–3216
208. Dutriez T, Borras J, Courtiade M, Thiébaut D, Dulot H, Bertoncini F, Hennion M-C (2011) J Chromatogr A 1218:3190–3199
209. Ávila BMF, Aguiar A, Gomes AO, Débora A, Azevedo DA (2010) Org Geochem 41:863–866
210. Dutriez T, Courtiade M, Thiébaut D, Dulot H, Bertoncini F, Vial J, Hennion M-C (2009) J Chromatogr A 1216:2905–2912
211. Mao D, Lookman R, van de Weghe H, Weltens R, Vanermen G, de Brucker N, Diels L (2009) Chemosphere 77:1508–1513
212. Adam F, Bertoncini F, Dartiguelongue C, Marchand K, Thiébaut D, Hennion M-C (2009) Fuel 88:938–946
213. Mao D, Lookman R, van de Weghe H, Weltens R, Vanermen G, de Brucker N, Diels L (2009) Environ Sci Technol 43:7651–7657
214. Adam F, Bertoncini F, Coupard V, Charon N, Thiébaut D, Espinat D, Hennion M-C (2008) J Chromatogr A 1186:236–244
215. Samuelarey J, Nelson RK, Reddy CM (2007) Environ Sci Technol 41:5738–5746
216. Samuelarey J, Nelson RK, Reddy CM (2007) Environ Sci Technol 41:5747–5755